



This discussion paper is/has been under review for the journal Atmospheric Chemistry and Physics (ACP). Please refer to the corresponding final paper in ACP if available.

The magnitude and causes of uncertainty in global model simulations of cloud condensation nuclei

L. A. Lee¹, K. J. Pringle¹, C. L. Reddington¹, G. W. Mann¹, P. Stier²,
D. V. Spracklen¹, J. R. Pierce³, and K. S. Carslaw¹

¹Institute for Climate and Atmospheric Science, School of Earth and Environment, University of Leeds, Leeds, UK

²Department of Physics, University of Oxford, Oxford, UK

³Department of Atmospheric Science, Colorado State University, Fort Collins, Colorado, USA

Received: 4 February 2013 – Accepted: 12 February 2013 – Published: 8 March 2013

Correspondence to: L. A. Lee (l.a.lee@leeds.ac.uk)

Published by Copernicus Publications on behalf of the European Geosciences Union.

ACPD

13, 6295–6378, 2013

Global CCN
uncertainty

L. A. Lee et al.

Title Page

Abstract

Introduction

Conclusions

References

Tables

Figures

◀

▶

◀

▶

Back

Close

Full Screen / Esc

Printer-friendly Version

Interactive Discussion



Summary of Comments on Global CCN uncertainty

Page: 6296

 Number: 1 Author: reviewer Subject: Sticky Note Date: 2013-05-02 12:24:12
Abstract could be somewhat shortened by leaving out technical details.

important for CCN uncertainty somewhere on the globe. The results lead to several recommendations for research that would result in improved modelling of cloud-active aerosol on a global scale.

1 Introduction

5 Successive Intergovernmental Panel on Climate Change (IPCC) reports have identified aerosol direct and indirect effects on climate as the largest uncertainty in the assessment of anthropogenic forcing (Schimel et al., 1996; Penner et al., 2001; Forster et al., 2007). Global aerosols can impact the climate in two distinct ways: The direct radiative effect is a result of atmospheric aerosols reflecting or absorbing solar radiation and
10 thereby cooling or warming the climate system. The indirect effect refers to the many ways in which aerosols interact with clouds, leading to changes in droplet concentrations, cloud albedo and precipitation (Lohmann and Feichter, 2005).

In response to the persistent uncertainty in aerosol forcing assessments, global aerosol microphysics models have been developed to more realistically describe the evolution of size-resolved aerosol properties, which determine the complex interactions
15 between aerosols, clouds and the climate (Binkowski and Shankar, 1995; Jacobson, 1997; Whitby and McMurry, 1997; Ackermann et al., 1998; Ghan et al., 2001; Adams and Seinfeld, 2002; Lauer et al., 2005; Liu et al., 2005; Stier et al., 2005; Spracklen et al., 2005a, 2008; Debry et al., 2007; Mann et al., 2012; Zhang et al., 2012). These models are more complex than have been used in Coupled Model Intercomparison
20 Project (CMIP) assessments (whose results feed into IPCC assessments) because they attempt to simulate the microphysical processes that determine the aerosol particle size distribution and composition on a global scale. In principle, this development in model sophistication should improve model fidelity, but the increased complexity has led to an increase in the number of uncertain model parameters, many of which
25 have very weak observational constraints and an incomplete scientific understanding (Ghan and Schwartz, 2007). Computational constraints have also restricted the grid



the uncertainty, which risks making model development an ad hoc process rather than one driven by the desire to reduce the persistent uncertainty in aerosol forcing.

Very few studies have attempted to quantify the parametric uncertainty of a single global aerosol model because of the computational expense. The first uncertainty analysis of the aerosol indirect effect was carried out by Pan et al. (1997) using the probabilistic collocation method to produce an approximation to their computer model in order to make uncertainty analysis feasible. Ackerley et al. (2009) studied the climate responses to changes in several sulphate aerosol parameters as part of the climateprediction.net project (Frame et al., 2009) with a simpler aerosol scheme than we use here. More recently, Haerter et al. (2009) studied the parametric uncertainty in aerosol indirect radiative forcing based on 7 cloud-related parameters with the ECHAM5 model. Lohmann and Ferrachat (2010) examined the parametric uncertainty effects on the climate in a global aerosol model by systematically varying 4 cloud parameters at specified values following a factorial design with 168 model runs. Lohmann and Ferrachat (2010) showed a parametric uncertainty in aerosol-climate effect of 11 % when considering the uncertainty in the four cloud parameters. Another approach to understanding uncertainty is to use the adjoint of the model, which has been applied to CCN in Karydis et al. (2012). Sensitivity analysis of cloud-aerosol interactions has been carried out by Markov Chain Monte Carlo simulations using an inverse modelling approach in Partridge et al. (2012). The approaches require either a very large number of model simulations in a Monte Carlo type approach (Ackerley et al., 2009) or a specific experimental design such as the factorial approach (Lohmann and Ferrachat, 2010), both of which are feasible only for a small number of parameters. However, the latest generation of global aerosol microphysics models have many tens of uncertain parameters. In order to make a realistic assessment of the spread in model simulations a more efficient statistical approach is required.

In our previous work we have demonstrated that Gaussian process emulators and variance-based sensitivity analysis can be used to study the sensitivity of global cloud condensation nuclei across the full uncertainty space of 8 microphysics parameters

Global CCN uncertainty

L. A. Lee et al.

Title Page

Abstract

Introduction

Conclusions

References

Tables

Figures

◀

▶

◀

▶

Back

Close

Full Screen / Esc

Printer-friendly Version

Interactive Discussion



 Number: 1 Author: reviewer Subject: Highlight Date: 2013-05-02 12:24:12

 Number: 2 Author: reviewer Subject: Highlight Date: 2013-05-02 12:24:12

 Number: 3 Author: reviewer Subject: Sticky Note Date: 2013-05-02 12:24:12
The authors are hence attempting to explore the statistics of a 28-dimensional parameter space.

 Number: 4 Author: reviewer Subject: Highlight Date: 2013-05-02 12:24:12

ters and their physical meaning in the model. In Sect. 5 we show the validation of the emulators. The results are presented in Sect. 6 in terms of the uncertain parameters and different global regions.

2 Statistical methods

To quantify the effect of parametric uncertainty on model simulations we apply well-established statistical methods to the global 3-D aerosol model. The overall approach is shown in Fig. 1, and consists of several distinct steps: First, expert elicitation is used to choose the uncertain model parameters and represent the uncertainty in these parameters as a probability distribution. Second, statistical design is used to choose an appropriate number of model runs to explore the parameter uncertainty space. Third, Gaussian process emulation is used to estimate model output throughout the entire parameter uncertainty space. A Bayesian framework is used to combine expert prior beliefs on parameter uncertainty and model behaviour with model runs to produce a posterior distribution of model simulations to make global sensitivity analysis possible. Finally, a full variance-based sensitivity analysis is carried out using the emulator to quantify the sensitivity of model simulations to the parameters and their interactions conditional on the emulator and the elicited parameter probability distributions. In essence, we are using emulators conditioned on the GLOMAP output to generate continuous model output across the parameter uncertainty space. The emulator can then be used for a Monte Carlo-type sampling of the output to generate sufficient data to enable a full variance-based sensitivity analysis.

2.1 Elicitation

2.1.1 General principles of elicitation

Elicitation provides a framework to formally represent the uncertainty in model parameters from several experts in the relevant field into a probability distribution (O'Hagan

Title Page

Abstract

Introduction

Conclusions

References

Tables

Figures

◀

▶

◀

▶

Back

Close

Full Screen / Esc

Printer-friendly Version

Interactive Discussion



Number: 1 Author: reviewer Subject: Sticky Note Date: 2013-05-02 12:24:12

I appreciate the authors attempt at providing the most "unbiased" assessment of possible parameter ranges, a difficult or perhaps impossible task.

The elicitation of experts, at any rate, is not an objective quantification of uncertainty in the parameters of interest. Experts themselves, while equipped with expertise and intuition, may make guesses on parameter ranges based on what they know to give "best" comparison between model output and observations. In this sense, an expert may even underestimate the possible range of parameters, as an expert opinion may involve more knowledge of what is the "proper" value to choose. Whether or not the expert choices reflect adequately the true parameter uncertainty can not be proven rigorously. This should perhaps be pointed out at this stage.

2.1.2 Conduct of the elicitation exercise

In this study the elicitation involved six aerosol modelling experts and a statistician. The quartile method of elicitation was chosen from those in Oakley and O'Hagan (2010) following a trial with known true answers, such as the distance from Leeds to London. The experts were given a few weeks to decide on the uncertain parameters to study and to gather evidence. The experts then discussed the uncertain parameters with some in a single office and others by teleconference. The range of each of the uncertain parameters was decided first and then the shape determined by cutting the range into regions of 50 % probability and then the two halves further into 50 % probability. The result of the cutting process was 4 regions all believed to contain 25 % of the probability of each parameter. Throughout the elicitation the experts were shown how the shape of the probability distributions was impacted by the decisions they made regarding the regions of probability. Visualising the probability distributions proved a valuable way of assessing the choices made by the experts. The discussions showed that some parameters were quite uncertain to all experts so the uncertainty ranges were quite wide whilst others could be constrained by expert knowledge and evidence. The experts chose initially 37 parameters. An initial study of 5 months of the data following the same method presented here was used to eliminate 9 parameters, resulting in 28 parameters to include in the final study. The probability distributions for the 28 final parameters were agreed by all experts after feedback. The experts were very confident in the ranges of the parameters even when the shape of the distribution was less certain. The details of the chosen parameters and their uncertainty distributions is given in Table 1.

2.1.3 Statistical design of the model runs

In order to build emulators of GLOMAP gridded output, 168 model runs were carried out using parameter settings sampled from a maximin Latin hypercube covering the uncertainty ranges of the 28 parameters in Table 1. Latin hypercube sampling splits the

 Number: 1 Author: reviewer Subject: Comment on Text Date: 2013-05-02 12:24:12

168 model runs seems like a fairly small number of simulations to adequately sample a 28-dimensional parameter space. Are all partial derivatives w.r.t. the individual parameters low-order functions (linear or quadratic) in the respective parameter ranges, so that sampling so few parameter sets can give a meaningful sample?

 Number: 1 Author: reviewer Subject: Comment on Text Date: 2013-05-02 12:24:12

Are all parameters sampled linearly, i.e. the range is cut into equal pieces or are some parameters sampled logarithmically? If all are linearly sampled, this means that each parameter is sampled from a uniform distribution between the two extreme values of the parameter. Is this adequate for all parameters? Why?

Number: 1 Author: reviewer Subject: Sticky Note Date: 2013-05-02 12:24:12

If only half of the model runs were used to produce the emulator, would similar results be obtained? I.e. did the authors check whether the data provided by the 168 runs is sufficient to allow a construction of the emulator?

where

$$\mathbf{H}^T = (h(\mathbf{x}_1), \dots, h(\mathbf{x}_n)), \quad (4)$$

$$\mathbf{A} = \begin{pmatrix} 1 & c(\mathbf{x}_1, \mathbf{x}_2) & \dots & c(\mathbf{x}_1, \mathbf{x}_n) \\ c(\mathbf{x}_2, \mathbf{x}_1) & 1 & & \vdots \\ \vdots & & \ddots & \\ c(\mathbf{x}_n, \mathbf{x}_1) & \dots & & 1 \end{pmatrix}, \quad (5)$$

and

$$\hat{\sigma}^2 = \frac{\mathbf{y}^T (\mathbf{A}^{-1} - \mathbf{A}^{-1} \mathbf{H} (\mathbf{H}^T \mathbf{A}^{-1} \mathbf{H})^{-1} \mathbf{H}^T \mathbf{A}^{-1}) \mathbf{y}}{n - q - 2} \quad (6)$$

where n is the number of training runs and q is the number of elements in $\boldsymbol{\beta}$ which depends on the prior choice of h in Eq. (1).

The choice of Gaussian process prior means that the posterior probability conditioned on the training data runs will also be a Gaussian process distribution which can be specified by a mean function and a covariance function. The posterior Gaussian process is a result of standard conditional multivariate Gaussian theory therefore the mean function is given by

$$m^*(\mathbf{x}) = h(\mathbf{x})^T \hat{\boldsymbol{\beta}} + t(\mathbf{x})^T \mathbf{A}^{-1} (\mathbf{y} - \mathbf{H} \hat{\boldsymbol{\beta}}), \quad (7)$$

which ensures that the function passes through each of the training data points and the posterior covariance function is

$$\hat{\sigma}^2 c^*(\mathbf{x}, \mathbf{x}') = \hat{\sigma}^2 (c(\mathbf{x}, \mathbf{x}') - t(\mathbf{x})^T \mathbf{A}^{-1} t(\mathbf{x}') + (h(\mathbf{x})^T - t(\mathbf{x})^T \mathbf{A}^{-1} \mathbf{H}) (\mathbf{H}^T \mathbf{A}^{-1} \mathbf{H})^{-1} (h(\mathbf{x}')^T - t(\mathbf{x}')^T \mathbf{A}^{-1} \mathbf{H})^T), \quad (8)$$

where

$$t(\mathbf{x})^T = (c(\mathbf{x}, \mathbf{x}_1), \dots, c(\mathbf{x}, \mathbf{x}_n)) \quad (9)$$

ensuring that the variance is zero at the training data points.

This mean of the posterior distribution is used as an approximation for the computer model and sampling from it provides the data we need for sensitivity analysis. If, after performing the model simulations, it is decided that the range or distribution of a parameter is narrower than the maximum elicited range, then the emulator can be sampled again without the need for more model runs. The covariance of the posterior distribution tells us how much uncertainty is due to using emulation rather than direct simulation of the computer model. Sampling many possible functions from the posterior distribution and comparing them to the mean function will provide us with information on how robust our results are and will form part of the emulator validation in Sect. 5.

2.2.2 Emulation of GLOMAP CCN

The emulation is carried out using the R package DiceKriging (Roustant et al., 2012). The model output y is the monthly mean CCN for each model grid cell and the model parameters \mathbf{x} and their ranges are given in Table 1 and described in detail in Sect. 4. An emulator is built for every month and every model grid cell. In every emulator our prior beliefs assume the modelled CCN can be estimated by a simple linear regression of the parameters and therefore $h(\mathbf{x}) = (1, x_1, \dots, x_{28})^T$ and $q = 29$ ($p+1$). The covariance structure is assumed to depend on the distance between each pair of parameter sets with a Gaussian function and therefore $c(\mathbf{x}, \mathbf{x}') = \sum_{i=1}^{p=28} \left(\frac{x_i - x'_i}{\delta_i}\right)^2$. The emulation depends on smoothness in the modelled monthly mean CCN response to each of the 28 parameters δ_i for $i = 1, \dots, 28$ which is calculated by maximum likelihood estimation. Model smoothness means that we have information on all model simulations in a neighbourhood close to those where the CCN concentrations have been calculated by running GLOMAP. If there are discontinuities in the model the emulator will not deal with these so alternative approaches would have to be found. It is reasonable to assume no sudden jumps in the monthly mean CCN within a single grid cell within the parameter uncertainty space (and finding such jumps if they exist is crucial if reliable



estimates of CCN concentration are to be predicted by the model). The hyperparameters of the mean function (β) and the covariance functions (σ and δ) are calculated by maximum likelihood of the training data as shown previously but if there is reason to believe their values are known they can be used directly. In most cases there is no strong prior information on the hyperparameters so it is often necessary to use the weak priors as we do here. The assumptions of linear mean and Gaussian correlation can be changed if more information is available or when an emulator is not well validated.

2.3 Variance-based sensitivity analysis

Variance-based sensitivity analysis is used to decompose the uncertainty in the model simulations to the uncertainty in each of the model parameters (Saltelli et al., 2000). The approach is able to quantify the sensitivity to each of the model parameters and their interactions (in the case of independent parameters) which cannot be done using the often applied one-at-a-time (OAT) studies. In a complex system such as the global aerosol cycle, interactions between uncertain parameters are thought to be likely and the effect of these interactions can be studied with the variance-based sensitivity analysis. The total variance of the CCN in each grid box is calculated by sampling from the emulator mean function shown in Eq. (7) given the uncertainty distributions in each of the 28 parameters obtained by the elicitation exercise.

With Y and \mathbf{X} defined as in Sect. 2.2.1 the emulator is used to estimate the variance (or uncertainty) around the mean Y due to the uncertainty in \mathbf{X} , $V = \text{Var}\{E(Y|\mathbf{X})\}$. With independent parameters \mathbf{X} , as we have here, the variance can be decomposed into its individual components, $V = V_i + V_j + \dots + V_m + V_{i,j} + \dots + V_{i,j,\dots,m}$, where $V_p = \text{Var}\{E(Y|\mathbf{X}_p)\}$ and $V_{p,q} = \text{Var}\{E(Y|\mathbf{X}_{p,q})\}$ represents the variance due to the interaction effect of parameters p and q , and so on. With an accurate emulator these estimates will be close to their true values.

In this study we use the extended-FAST method (Saltelli et al., 1999) in R package sensitivity (Pujol et al., 2008) to sample from the emulator mean function and decom-

Title Page

Abstract

Introduction

Conclusions

References

Tables

Figures

◀

▶

◀

▶

Back

Close

Full Screen / Esc

Printer-friendly Version

Interactive Discussion



 Number: 1 Author: reviewer Subject: Comment on Text Date: 2013-05-02 12:24:12
Again, how would the interaction, i.e. correlation, between parameters vary, if fewer than the 168 model runs were used in the assessment?

pose the total variance in CCN into its parametric sources. The extended-FAST method provides a more efficient sampling from the parameter uncertainty space than Monte Carlo sampling designed specifically for sensitivity analysis. Two measures of sensitivity are calculated in the first instance. These are the main effect index and total effect index. The main effect index measures the percentage of the total variance that will be reduced if parameter p can be learnt precisely, V_p/V . The total effect index measures both the individual effect and the interaction effect of each parameter with all others as a percentage of the total variance, V_{T_p}/V where V_{T_p} represents all variance components including parameter p . The two sensitivity measures are compared to assess the sensitivity of the model output to interactions. If there are no interactions with parameter p $V_p = V_{T_p}$.

3 Model description and set-up

The GLObal Model of Aerosol Processes (GLOMAP-mode) (Mann et al., 2010) is an aerosol microphysics module that simulates evolution of the size distribution and composition of aerosol particles on a global 3-D domain. The model has been used in several studies of global aerosol (Schmidt et al., 2010, 2011, 2012; Woodhouse et al., 2010, 2012; Spracklen et al., 2011b; Lee et al., 2012; Mann et al., 2012) and is a faster version of the GLOMAP-bin module that has been very widely used (e.g. Spracklen et al., 2005a,b, 2010, 2011a; Korhonen et al., 2008; Reddington et al., 2011). Both models have been compared and evaluated against observations in Mann et al. (2012).

Here, the aerosol model is run within the TOMCAT global 3-D offline chemistry transport model (CTM) (Chipperfield, 2006). The same GLOMAP-mode module is also implemented within a general circulation model (Bellouin et al., 2012), being the aerosol component of the UK Chemistry and Aerosol (UKCA) sub-model of the Hadley Centre Global Environmental Model. In a CTM the aerosol and chemical species are transported and mixed by 3-D meteorological fields read in from analyses, here from the European Centre for Medium-Range Weather Forecasts ERA-40 reanalyses (Uppala

Title Page

Abstract

Introduction

Conclusions

References

Tables

Figures

◀

▶

◀

▶

Back

Close

Full Screen / Esc

Printer-friendly Version

Interactive Discussion



Number: 1 Author: reviewer Subject: Sticky Note Date: 2013-05-02 12:24:12

It would be good to further strengthen the robustness of the statistical results and the construction of the emulator. One way in doing this could be to use a sub-sample of the data and investigate the shift of the obtained results.

provide a complete picture of the importance for cloud drop formation in all clouds. Our choice of $CCN = N_{50}$ is equivalent to a supersaturation of about 0.3% and is typical of values reached in stratocumulus updraught cells. If we assumed a higher supersaturation (smaller diameter of activation) then CCN would become more sensitive to processes that determine the concentration of smaller particles, and vice versa for lower supersaturations.

4 Description of uncertain parameters and model experiments

4.1 Parameters and their meaning

As described in Sect. 2, following expert elicitation, a total of 28 uncertain model parameters were identified for the perturbed parameter ensemble. The parameters relate to microphysical processes, emissions of precursor gases and primary particles, and the structure of the aerosol model (assumptions made about the representation of the size distribution). The parameters are summarised in Table 1. Although some parameters (e.g. wildfire emissions) are likely to be better constrained in some regions than others, we have varied each parameter uniformly over the whole global 3-D domain, with the chosen uncertainty reflecting an upper limit for the range of their variation or uncertainty. Regional variations in the uncertainties could be studied by introducing separate parameters for each region, but we have not done this. The effect of a smaller range can be studied by adjusting the assumed distribution of a parameter after emulation.

4.1.1 Definition of microphysical process parameters

Nucleation rates (P1 and P2). Throughout the atmosphere we use the binary homogeneous H_2SO_4 - H_2O nucleation (BHN) rate model of Vehkamäki et al. (2002) scaled by a factor that varies between 0.01 and 10. Zhang et al. (2010) have compared a large number of nucleation rate expressions under prescribed conditions. However, our previous studies (Spracklen et al., 2005a,b; Mann et al., 2010) show that in our model

 Number: 1 Author: reviewer Subject: Comment on Text Date: 2013-05-02 12:24:12

Does this factor vary homogeneously, i.e. what is the distribution it varies by? What is the motivation behind choosing a cutoff of 0.01, why not 0.1 or 0.001? For a uniform sampling, the value of the cutoff should probably be irrelevant, but in many cases the outcome depends sensitively on the sampling ...

be wet scavenged or undergo cloud processing, which adds sulphate mass to the particles (see parameter 8). Only particles in the soluble modes (larger than 50 nm equivalent dry diameter) are counted as CCN. This approach (developed by Wilson et al., 2001) is a simplification of a complex process in which multiple factors can affect the water-solubility of the particles and their activation into cloud drops, but is widely used in global models (e.g. Stier et al., 2005; Spracklen et al., 2006).

Activation diameter (P4). The GLOMAP-mode version used here follows the approach for activation used by Spracklen et al. (2005a), whereby particles larger than a prescribed dry-diameter are able to activate to cloud drops. A single value of activation diameter is used globally in a given run. In reality, the activation diameter depends on updraught speed (usually not diagnosed in models), particle composition, and the size distribution (Nenes and Seinfeld, 2003; Pringle et al., 2009), and is therefore likely to vary spatially. However, this is a computationally expensive process to simulate, with large uncertainties in the driving variables (such as unresolved cloud-scale updraughts applied over large global grid boxes). In GLOMAP, the activation diameter controls the formation of cloud drops in all low-level clouds, which we assume are non-precipitating (see Fig. 2a). Thus it mainly controls which particles undergo cloud processing (sulphate production on the particles due to oxidation of SO₂ during the existence of cloud), and therefore how the size distribution is affected by clouds.

Droplet pH controlling in-cloud SO₄ production from SO₂+O₃ (P5 and P6). The rate of the reaction SO₂ + O₃ → SO₄ is controlled by the pH of cloud water (Gurciullo and Pandis, 1997; Kreidenweis et al., 2003) and has been identified as an important uncertainty in the global sulphur cycle (Faloona, 2009). We assume this reaction occurs in low-level clouds (Fig. 2a) but not in deep precipitating or frontal clouds in which the formed sulphate is rapidly removed. The pH is assumed to be the controlling parameter, which leads to a change in rate by a factor 10⁵ for pH between 3 and 6 (Seinfeld and Pandis, 1998). One pH parameter is used for clean (lower acidity)

Title Page

Abstract

Introduction

Conclusions

References

Tables

Figures

I◀

▶I

◀

▶

Back

Close

Full Screen / Esc

Printer-friendly Version

Interactive Discussion



Scavenging efficiency in ice-containing clouds (P8). This parameter controls the fraction of particles accessible to nucleation scavenging when air is below -10°C (i.e. scavenging affects only a fractions of the aerosol in a given time step). Our previous work has shown this parameter to be important in the Arctic (Korhonen et al., 2008; Browse et al., 2012). We treat this parameter as separate from warm cloud effects because ice cloud scavenging can affect the seasonal cycle of Arctic aerosol (Browse et al., 2012).

Dry deposition of Aitken and accumulation mode particles (P9 and P10). GLOMAP calculates the wind speed and size-dependent deposition velocity due to Brownian diffusion, impaction and interception according to Slinn (1982) using resistances from Zhang et al. (2001) and three land-surface types: ocean, forest and other. In the perturbed runs, the calculated dry deposition velocity in each time step over each surface type is scaled for each particle size by a given factor. Taking into account the difficulty of applying dry deposition mechanisms to large global grid boxes containing unresolved inhomogeneity, we assume large uncertainties in the deposition velocity of a factor 10 for the accumulation mode particles (Giorgi, 1988).

4.1.2 Definition of size distribution structural parameters

Accumulation and Aitken mode widths (P11 and P12). GLOMAP-mode uses fixed geometric widths of the log-normal size distribution modes (defined by the standard deviation of the distribution). Observations show that the width can vary in time and space (Heintzenberg et al., 2000, 2004; Birmili et al., 2001). However, allowing for dynamically evolving mode widths adds to the complexity of the model and is therefore not widely adopted in global models. The chosen uncertainty ranges of the Aitken and accumulation mode widths were based mainly on Heintzenberg et al. (2004) and Birmili et al. (2001). The same widths were applied for soluble and insoluble particles. Changing the mode width modifies the size distribution for particles in that mode,

5 *Fossil fuel, biofuel and biomass burning particle emission sizes (P18, P19 and P20).* These parameters directly control the number of emitted particles for a given mass flux, and therefore directly influence the CCN population. The size of the emitted particles is not reported in emissions inventories, but is needed for size-resolving models, and is a major uncertainty in previous model studies of CCN (e.g. Merikanto et al., 2009; Reddington et al., 2011; Spracklen et al., 2011a). For the AEROCOM prescribed emissions experiment, Dentener et al. (2006) made recommendations for the size distribution of primary emissions based on available information in the literature. They recommended finer sizes be used for fossil fuel combustion sources than for biofuel combustion and wildfire emissions. Although more recent measurements provide some information about emitted particle number concentrations (Janhäll et al., 2010), the particle size remains very uncertain. The size of fossil fuel combustion particles depends on the source. Biomass burning and wildfire particle size depends on burning efficiency (Janhäll et al., 2010) amongst other parameters, but these processes are not treated in global models.

20 *Sub-grid scale sulphate particle production (P21 and P22).* Two parameters describe the formation of particles in sub-grid scale plumes, such as power plants and degassing volcanoes (Mather et al., 2003; Luo and Yu, 2011; Stevens et al., 2012). P21 defines the fraction of the SO₂ mass that enters the model grid square as new sulphate particles and P22 defines the size of these particles (and hence their number concentration for fixed mass). The particles are most likely formed by nucleation and growth. Previous studies have shown this to be an important source of global CCN (Spracklen et al., 2005b; Pierce and Adams, 2006; Luo and Yu, 2011), but other studies suggest a more limited effect (Stier et al., 2006). We base our ranges on the plume-scale study of Stevens et al. (2012).

25 *Sea spray particle mass flux (P23).* We account for uncertainties in the wind-driven mass flux of sea spray particles in the size range 35 nm to 20 µm dry diameter

5 Validation of the emulator

Figures 3 and 4 show the validation of the emulator. Scatter plots of the emulator estimates versus the GLOMAP validation runs at various grid box locations are shown in Fig. 3, with the 95 % confidence intervals around the emulator mean calculated using Eq. (8). Figs. 4a, c shows maps of the January and July global emulator validation in terms of the percentage of GLOMAP validation runs that lie within the 95 % confidence interval of the emulator estimate. In most grid cells over 90 % of the GLOMAP validation simulations lie within the 95 % confidence interval of the emulator. Note that the mean emulator estimate is used for the Monte-Carlo-type sampling (Sect. 2.3), and Fig. 3 shows that the emulator mean CCN is very close to the GLOMAP simulation, shown by the 1 : 1 line.

If the emulator is to be useful then the uncertainty needs to be less than the parametric uncertainty that we are aiming to quantify. The emulator uncertainty is compared to the parametric uncertainty in Figs. 4b, d. The emulator uncertainty was calculated as the standard deviation around the mean of 10 000 Gaussian process functions sampled from the emulator (Eqs. 7 and 8). Figure 4b, d shows that the emulator uncertainty is less than 10 % of the parametric uncertainty.

The validity of the emulator can also be assessed subjectively by examining the maps of parametric uncertainty (next section). The CCN and sensitivity maps are produced from an analysis of 8192 independent emulators (one for each grid cell) and yet we find that the spatial patterns can be readily understood in terms of the driving processes, implying that the emulator mean is not dominated by its uncertainty in the different grid boxes. There may be grid boxes that are less well emulated but for the purpose of our global analysis the emulators here are considered valid.

6 Results

6.1 Metrics of uncertainty

We describe the results in terms of three measures of uncertainty.

The *standard deviation* of the CCN probability distribution in each grid cell provides a direct measure of the absolute uncertainty in CCN caused by the uncertain parameters. It is calculated as the square root of the total variance due to the uncertainty in the 28 parameters (see Sect. 2.3). Figure 5 shows January and July maps of emulator-estimated CCN and the standard deviation, while Fig. 6 gives some examples of the probability distribution of CCN for selected locations, from which the standard deviation was calculated. We also carry out a variance-based sensitivity analysis to quantify the contribution of each parameter i to the variance in the modelled CCN. These parameter effect variances can also be mapped (Lee et al., 2012). Here we show maps of the $1\sigma_{\text{CCN}}$ uncertainty in CCN ($\sigma_{\text{CCN},i} = \sqrt{V_{\text{CCN},i}}$ for parameter i). The $\sigma_{\text{CCN},i}$ value is the square root of the main effect index times the total variance for parameter i (see Sect. 2.3). The $\sigma_{\text{CCN},i}^2$'s cannot be added to obtain the total uncertainty in Fig. 5 unless there is zero interaction between the parameters.

The coefficient of variation or *relative uncertainty* is the standard deviation divided by the emulator mean CCN ($\sigma_{\text{CCN},i}/\mu_{\text{CCN}}$). This is shown also in Fig. 7. Relative uncertainty is a more appropriate measure of uncertainty in CCN than absolute uncertainty because the uncertainty in cloud reflectivity depends approximately on the ratio of change in cloud drop number (CDN) concentration to absolute concentration ($\Delta\text{CDN}/\text{CDN}$), termed the susceptibility (Twomey, 1991). Although CCN and CDN concentrations are not linearly related, the relative uncertainty is more relevant for climate than the absolute uncertainty. For other quantities, like black carbon mass concentrations, the direct aerosol effect depends approximately linearly on column mass, so the absolute uncertainty in BC would be more relevant.



The *fraction of variance* explained by a parameter is the reduction in variance that would be obtained if a particular parameter were known precisely. A parameter with a large contribution to variance may have its effect in a region with overall low variance. It is therefore a measure of local “research priority” (improved knowledge of highly ranked parameters would lead to a greater reduction in uncertainty in CCN) but not directly relevant to the impact on clouds and climate. Thus, information on CCN relative uncertainty and fraction of variance can be used together to estimate the effect of an uncertain parameter on climate and to identify the most important parameter in terms of reducing the uncertainty in the model.

6.2 Magnitude of uncertainty in global CCN

Figure 5 shows that the standard deviation correlates well with mean CCN concentrations but this is not the case for the relative uncertainty. In general, the relative uncertainty is lower at low latitudes than at high latitudes, although there are exceptions in the biomass burning regions. It varies between a minimum of about $\pm 30\%$ in many clean marine regions to about $\pm 40\text{--}100\%$ over land areas and at high latitudes. The peak $1\sigma_{\text{CCN}}$ reaches about 80% over the January Arctic and July Antarctic. There is a clear seasonal cycle in relative uncertainty in parts of the NH. For example, winter-time NH marine regions reach about $30\text{--}50\%$ but generally less than 30% in summer. Peaks in uncertainty at summer high latitude continental locations are associated with large uncertainties in wildfires, as we show below.

Although we do not attempt to compare the model uncertainties with observed CCN, it is worth noting that in general the spread of the model simulations is less than shown in the only compilation of global CCN measurements (Spracklen et al., 2011a). In that study the $1\sigma_{\text{CCN}}$ range in modelled minus observed CCN was at least 100% . Some of this model-observation scatter may be due to poor collocation of the modelled and observed concentrations.

 Number: 1 Author: reviewer Subject: Comment on Text Date: 2013-05-02 12:24:12

It seems that the authors have varied all 28 parameters independently. It could then be that by sampling such a large number of parameters, on average a compensation of effects will occur in terms of the value of CCN. The authors are encouraged to explain if (and why) the sampling for the 28 parameters was done independently and what the statistical effects of independent variation are.

6.3 Factors controlling uncertainty in CCN

The variance-based sensitivity analysis was carried out on each model grid box separately. Figure 7 shows the global distribution of the absolute and relative CCN uncertainty and Fig. 8 shows a global summary of the ranked relative uncertainties. The ranked bar charts were calculated by globally averaging $\sigma_{CCN,i}/\mu_{CCN}$ over all grid boxes at 915 hPa, including a weighting for grid box area. We also stratify the global data into clean/polluted according to the black carbon concentration (clean $< 50 \text{ ng m}^{-3}$, polluted $> 100 \text{ ng m}^{-3}$) (Fig. 8c) and by weighting $\sigma_{CCN,i}/\mu_{CCN}$ by cloud fraction based on the International Satellite Cloud Climatology Project (ISCCP) global D2 all-cloud data (Rossow and Schiffer, 1999) (Fig. 8d). The cloud fraction is shown in Fig. 2a. Figure 8a, b also distinguish parameters according to whether they describe processes, emissions, model structures, or a combination of processes and emissions (the two SOA-related parameters). These global mean bar charts summarise the global importance of parameters.

There are several things to keep in mind when comparing these uncertainty maps. First, the importance of a parameter does not necessarily imply that the associated process or emission is acting locally. For example, the activation diameter in clouds accounts for a large fraction of the uncertainty over Antarctica, although there are no clouds there. This implies that the process is the dominant factor that affects the amount of aerosol transported to the region. Second, the importance of a parameter describes the effect it has on the uncertainty in aerosol, not necessarily how important it is for determining the absolute aerosol amount. For example, a low sensitivity to the Γ_T nucleation rate does not imply that Γ_T nucleation could be removed from the model; but only that, when it is included in the model, the aerosol is insensitive to the choice of rate within the range we have tested, that is, the process could possibly be simplified but not eliminated. Third, the contribution of a parameter to aerosol variance does not imply a positive association. For example, increases in biogenic SOA could lead

 Number: 1 Author: reviewer Subject: Comment on Text Date: 2013-05-02 12:24:12
has the acronym been defined?

 Number: 2 Author: reviewer Subject: Comment on Text Date: 2013-05-02 12:24:12

to decreases in CCN due to increases in aerosol surface area and suppression of nucleation.

Below we describe the factors controlling uncertainty in CCN first by parameter and then by region and season.

6.3.1 Uncertainty due to microphysical processes

Nucleation rates (P1 and P2). The peak effect of uncertainty in the rate of boundary layer nucleation on the CCN standard deviation is about $50\text{--}100\text{ cm}^{-3}$, or a maximum CCN relative uncertainty of 10% in any region. The fraction of variance is also generally less than 10%, highly localised over remote parts of summertime Canada, the European boreal forest, the Arctic, South Africa and parts of Asia. The FT nucleation rate is a process of high importance to CCN (Merikanto et al., 2009) but relatively insensitive to the rate. The greatest contribution to the standard deviation is mostly over land areas, reaching a $1\sigma_{\text{CCN}}$ of $100\text{--}200\text{ cm}^{-3}$ and a peak relative uncertainty of about 25% at high latitudes, but generally less than 10%. The regions where the FT nucleation rate is most important do not coincide with regions where it makes the greatest contribution to nucleated CCN – over subtropical marine regions. Over clean regions the production of CCN is mainly through slow coagulation through the dry FT, making the CCN insensitive to the initial nucleation rate in the UT. Over polluted regions with higher vapour supply there is more condensational growth of the particles and a larger fraction survive to CCN, making the CCN in the BL more sensitive. Uncertainty in nucleation rates is relatively unimportant in our model in both clean and polluted regions.

Ageing (P3). Ageing makes a localised contribution to variance over biomass burning and other BC source regions, of up to 2000 cm^{-3} $1\sigma_{\text{CCN}}$ uncertainty in regions with very high CCN of 5000 cm^{-3} . However, the relative uncertainty is typically less than 10% in these regions and the fractional contribution to variance is everywhere less than 5%. This low sensitivity is partly because of the much larger effect of

6325

Title Page

Abstract

Introduction

Conclusions

References

Tables

Figures

◀

▶

◀

▶

Back

Close

Full Screen / Esc

Printer-friendly Version

Interactive Discussion



Title Page

Abstract

Introduction

Conclusions

References

Tables

Figures

I◀

▶I

◀

▶

Back

Close

Full Screen / Esc

Printer-friendly Version

Interactive Discussion



Nucleation scavenging diameter offset (P7). The size at which aerosol particles are scavenged in frontal and convective precipitation has a surprisingly small effect on CCN uncertainty at the 915 hPa level. As described in Sect. 4 the equivalent dry diameter at which activated aerosol particles are scavenged in precipitation is equal to the activation diameter (P4) plus the scavenging diameter offset. These results therefore show that CCN are more sensitive to the activation diameter (relative uncertainties exceeding 20 % in many areas) than they are to the scavenging diameter offset. The effect on standard deviation is concentrated over land areas, although the fractional contribution to uncertainty in CCN is never more than a few percent. The relative uncertainty is greatest over marine regions and the wintertime Arctic, but is everywhere less than about 20 %. Thus, it appears that at the altitude of cloud base, CCN concentrations are relatively insensitive to in-cloud nucleation scavenging assumptions, other than assuming all activated particles are scavenged. However, as we showed in Lee et al. (2012) the scavenging diameter becomes a dominant parameter throughout most of the FT.

Nucleation scavenging in ice clouds (P8). This parameter contributes only a few percent to the total variance in a few isolated locations with no clear pattern. It was expected that it would strongly influence Arctic CCN uncertainty (Browse et al., 2012) but the effect is much smaller than for aerosol mass concentrations highlighted in that study. There is a more consistent wintertime effect on BC, accounting for 10–30 % of BC variance in winter.

Dry deposition of Aitken and accumulation mode particles (P9 and P10). The effect of dry deposition on the standard deviation follows the changes in aerosol abundance, consistent with it being a first-order loss process. The dry deposition of accumulation mode particles is more important for CCN than Aitken mode, even though the rate is lower (primarily because CCN reside mostly in the accumulation mode). It is largest over land and on continental outflow regions. The map of relative

uncertainty is quite different, with a 10–30 % effect over almost all marine regions and a negligible contribution over almost all land areas. The fractional contribution to variance reaches ~30 % in regions where few other factors are important, such as in the tropics. Although dry deposition of accumulation mode particles is quite slow (particle lifetimes of up to several days), it is the dominant (or even sole) loss process of accumulation mode particles close to the surface in many regions. Unlike other processes and emissions, it is a first order loss process that occurs continuously and everywhere. Thus, globally averaged, it is an important factor in the relative uncertainty in CCN in the boundary layer. We also note the lack of precipitation.

6.3.2 Uncertainty due to size distribution parameters

Accumulation and Aitken mode widths (P11 and P12). The accumulation mode width has an effect over polluted NH regions, reaching a maximum relative uncertainty of 10 % in the wintertime Arctic. The width of the Aitken mode has a much more widespread absolute effect over NH polluted regions and hotspots in biomass burning area. The relative uncertainty in CCN reaches 30 % in the wintertime Arctic and 40 % over the Antarctic and parts of the Southern Ocean. As a fraction of total variance it accounts for 10–30 % over large regions of the ocean including the Arctic, thus the Aitken mode width is a structural parameter of high importance for reducing uncertainty in predicted CCN of 50 nm dry diameter. Figure 8c, d shows that the Aitken mode width is the second-most important uncertain parameter for CCN in clean and cloudy regions. The Aitken mode width is more important for CCN uncertainty than the accumulation mode width because almost all accumulation mode particles are counted as CCN, while the fraction of Aitken mode that is counted depends on how the distribution extends beyond the assumed CCN size of 50 nm dry diameter. This is the only parameter that has a significantly different impact on CCN uncertainty in cloudy versus non-cloudy regions.

Title Page

Abstract

Introduction

Conclusions

References

Tables

Figures

◀

▶

◀

▶

Back

Close

Full Screen / Esc

Printer-friendly Version

Interactive Discussion



(3) the rate of sulphate production in cloud drops, (4) dry deposition of the Aitken mode, and (5) the size of particles scavenged in precipitating clouds. The nucleation rate of new particles is less important and has a maximum effect on $\sigma_{\text{CCN}}/\mu_{\text{CCN}}$ of less than about 8% anywhere.

For size distribution representation, the Aitken mode width is clearly the number 1 parameter, with the other size distribution parameters being fairly unimportant.

The rank order of parameters is strongly dependent on the level of pollution, as defined by black carbon concentrations (Fig. 8c). There is an obvious reordering of the importance of the emissions of BC-containing particles (biomass, fossil fuel, biofuel emissions) in clean and polluted regions. But we also find that the sensitivity to natural emissions is strongly suppressed in polluted regions because of the high concentrations of anthropogenic aerosol. For example, between clean and polluted regions $\sigma_{\text{CCN}}/\mu_{\text{CCN}}$ decreases by a factor 4.5 for sea spray, a factor 4 for DMS and a factor 2 for volcanic SO_2 . This implies that pollution will have suppressed the importance of natural aerosol-climate feedbacks. Interestingly, anthropogenic SOA has a larger effect on $\sigma_{\text{CCN}}/\mu_{\text{CCN}}$ in clean regions than polluted regions (by a factor 3) because of its long-range transport.

Finally, we note that the rank order is essentially unchanged when the gridded $\sigma_{\text{CCN}}/\mu_{\text{CCN}}$ values are weighted by low-cloud fraction (Fig. 8d). This implies that the global rank importance of a parameter is also a good indicator of its importance for cloud drop formation and indirect forcing.

6.3.5 Relative importance of emissions, size distribution and processes

Figure 10 splits the contribution to uncertainty according to microphysical processes, size distribution representation and emissions, as coloured in Fig. 8a. The two SOA-related parameters (green in Fig. 8a) were included in both the processes and emissions group because they represent uncertainty in both the emissions of BVOCs and the chemistry of SOA formation.

Cape Grim. Cape Grim on the southern tip of Tasmania is an important site for the long-term monitoring of aerosols and trace gases (Ayers et al., 1986; Ayers and Gras, 1991) and has been used extensively for studies of marine aerosol processes. The key parameters controlling CCN variance at Cape Grim are very heterogeneous, but appear to be controlled mostly by continental emissions. The most obvious feature is the importance of biomass burning from March to May. But outside this period a mix of natural and anthropogenic aerosol parameters is important, with marine aerosols and precursors (sea spray and DMS) not being prominent among them. So although DMS emissions control the seasonal cycle of CCN at Cape Grim (Korhonen et al., 2008), CCN concentrations are much more sensitive to a range of other emissions (i.e. the seasonal cycle will still occur within the range of DMS emissions that we have used here). This result will have implications for interpreting any long term trends. However, care needs to be taken comparing with observations because of the strong land-sea gradient in aerosol properties at this site.

Mace Head. CCN uncertainty at this coastal site is similar to Cape Grim in being controlled by a wide range of parameters. The Mace Head site (Jennings et al., 1991) is assumed to be representative of the marine aerosol environment. However, the factors controlling CCN uncertainty in the global model are actually mainly pollution sources. One reason for the low importance of marine aerosol properties is that the site is in a model grid box that overlaps with the UK, although the agreement of our GLOMAP-bin model at this site does not suggest any particular issue with model skill (Reddington et al., 2011). An improved understanding of aerosol model uncertainty at this and other coastal sites may require filtering of the data to identify marine air masses, or analysis of model grid boxes over open ocean rather than on the coast.

Title Page

Abstract

Introduction

Conclusions

References

Tables

Figures

I◀

▶I

◀

▶

Back

Close

Full Screen / Esc

Printer-friendly Version

Interactive Discussion



7 Discussion and conclusions

We have used an ensemble of global aerosol microphysics simulations together with emulators and variance-based sensitivity analysis to quantify the magnitude and causes of uncertainty in monthly-mean CCN for every 2.8° grid box of a global aerosol model at the altitude of 915 hPa (approximately cloud base). Twenty-eight uncertain parameters and their likely uncertainty ranges were defined based on expert elicitation. A Gaussian Process emulator of the model behaviour across the 28-dimensional parameter space in each grid box enables a full probability density distribution of CCN to be generated by Monte Carlo-type sampling for each grid box based on only 168 model runs. The probability distributions then allow the standard deviation of modelled CCN to be computed on a global scale. A full variance-based sensitivity analysis was also conducted, which generates globally gridded information about the most important sources of uncertainty in modelled CCN.

This analysis of uncertainties in a global aerosol microphysics model points to several priorities for reducing parametric uncertainty in modelled CCN. The following statements refer to the relative uncertainty in CCN concentrations (> 50 nm dry diameter) in the boundary layer at 915 hPa, which we defined as the global mean of the standard deviation divided by the mean CCN in each grid box (Sect. 6.1). Figure 11 shows a schematic of the relative importance of the parameters we have studied, with the size of the font proportional to the relative uncertainty.

- The most important process for global mean CCN uncertainty is dry deposition of the accumulation mode. Dry deposition is a globally important process that occurs continuously and everywhere at a first order rate that scales with aerosol concentration. In contrast, many other processes are only regionally important, so are less prominent as a global mean uncertainty. The dry deposition velocity is also the parameter with the greatest uncertainty (factor 0.1 to 10). A more refined study could take account of differences in uncertainty over different land surface types, rather than the globally uniform uncertainty applied here.

factors. In general, the dependence is much less than this scaling would suggest, because smaller more numerous primary particles need to grow to CCN sizes.

- Sub-grid formation of sulphate particles in plumes is approximately as important for CCN uncertainty as the uncertainty in SO_2 itself, despite the fact that less than 1 % of the SO_2 is converted into particles in the plume. More research is needed to understand the formation and dispersion of particles in plumes (Stevens et al., 2012). So far, studies have focused only on sulphate particles. However, given the large uncertainty, it would be worth identifying whether sub-grid production of particles occurs in other environments.
- Biogenic secondary organic aerosol has a surprisingly small effect on CCN uncertainty, despite a very large range applied in the model (5 to 360 Tg a^{-1} SOA production). This low sensitivity of a secondary aerosol component contrasts with the much higher sensitivity of CCN to SO_2 emissions ($35\text{--}87 \text{ Tg a}^{-1}$). The likely reason for the different sensitivities is that H_2SO_4 from SO_2 oxidation produces new particles as well as growing existing ones, while SOA only grows existing particles in our model. An important area of research is therefore to understand how and to what extent biogenic SOA influences the nucleation of new particles. If it does, the large uncertainties associated with biogenic SOA might make it one of the most important parameters in global CCN production.
- Anthropogenic SOA has a larger effect on CCN uncertainty than biogenic SOA despite having a smaller overall parameter uncertainty ($3\text{--}160 \text{ Tg a}^{-1}$). With the approach we have taken, this parameter has an effect on CCN uncertainty approximately as great as sea spray and anthropogenic SO_2 emissions. Anthropogenic SOA uncertainty influences CCN mainly in winter and has a widespread hemispheric effect on CCN uncertainty, while biogenic SOA has a patchy continental effect. One reason for the greater impact on CCN may be that anthropogenic SOA forms in polluted regions where a large number of small particles can grow to CCN sizes. There are many open questions concerning anthropogenic SOA,

6341

Title Page

Abstract

Introduction

Conclusions

References

Tables

Figures

◀

▶

◀

▶

Back

Close

Full Screen / Esc

Printer-friendly Version

Interactive Discussion



- Emissions and processes are more important than the representation of the size distribution in the aerosol microphysics model. We previously showed that a bin and a modal model agree quite well in the simulations of many aerosol quantities. Some important structures can be improved, as noted below, but in general the development of more complicated and computationally demanding aerosol models to calculate varying mode widths should have lower priority than the improvement in model processes and emissions. The effect of structural changes in the host global transport model have not been assessed here, but AEROCOM intercomparisons suggest the variance could be large.
- The most important parameter representing the size distribution in a modal model in terms of simulation of CCN is the width of the Aitken mode. This parameter was varied between 1.2–1.8 and accounts for up to 40 % of variance in CCN in remote regions, particularly at high latitudes in winter. In terms of global mean relative uncertainty in CCN ($\sigma_{\text{CCN}}/\mu_{\text{CCN}}$) it is ranked second out of the 28 parameters we studied. It is important because it determines the fraction of Aitken particles that are counted as CCN at 50 nm dry diameter. It is important to note that the importance of this parameter would decrease if we considered larger CCN, although the width of the accumulation mode would then rank more highly. Mixing of different air masses with different mode widths cannot be handled in a modal model with constant width. Possible approaches to improvement include replacing the Aitken mode with bins, e.g. as in the SALSA model (Kokkola et al., 2008; Bergman et al., 2012) or developing a modal model with a prognostic treatment of the width of the modes, as previously suggested (e.g. Weisenstein et al., 2007). More climatological information on Aitken mode aerosol properties (Heintzenberg et al., 2000, 2004; Birmili et al., 2001) would be valuable for model evaluation.

We reiterate that these conclusions refer to the model factors that are important for the uncertainty in model simulations of CCN. They are the properties of the model that should be given most attention in efforts to reduce uncertainty. The important uncer-

Title Page	
Abstract	Introduction
Conclusions	References
Tables	Figures
◀	▶
◀	▶
Back	Close
Full Screen / Esc	
Printer-friendly Version	
Interactive Discussion	



tain factors may not be the same as those that account for the absolute abundance of aerosol. For example, SOA is a major component of the aerosol mass, but our model results have shown that CCN is not very sensitive to its formation, most likely because of how it affects other aerosol processes. Likewise, nucleation is known to be an important source of CCN (e.g. Spracklen et al., 2008; Makkonen et al., 2009; Merikanto et al., 2009; Yu and Luo, 2009) but CCN is not strongly sensitive to the nucleation rate.

Care needs to be taken to verify these model sensitivity results using observations. As we have pointed out in several cases, an uncertain model parameter can impact aerosol far away from where the emission or process occurred. The most obvious example of this effect is the importance of cloud processing for Antarctic CCN when there are no clouds over the Antarctic, which is caused by the integrated effect of in-cloud sulphate formation along air mass trajectories.

Nevertheless, the uncertainty information generated in this study provides the basis for a much more rigorous evaluation of the model against observations, leading to a more structured approach to model improvement. The normal approach in model evaluation and improvement is to reduce the bias between modelled and observed aerosol by tuning a small number of existing parameters or developing more sophisticated models for various processes of interest. With new information about the full probability distribution of the model and ranked parameter sensitivities in all grid boxes it will be possible to home-in on the most likely causes of model bias. Structural uncertainties can be more easily identified in cases where observations lie outside the confidence intervals of the model. Confronting these results with observations is therefore a high priority.

It is essential to extend the current study to include the structural uncertainty in the host transport model and the parametric uncertainty in the host model physics. An important question is whether the uncertainty in global aerosol stems largely from parametric uncertainty in the aerosol microphysics model or from uncertainty in the meteorological fields that transport and ultimately remove the aerosol. This study has

ACPD

13, 6295–6378, 2013

Global CCN uncertainty

L. A. Lee et al.

Title Page

Abstract

Introduction

Conclusions

References

Tables

Figures

◀

▶

◀

▶

Back

Close

Full Screen / Esc

Printer-friendly Version

Interactive Discussion



been conducted in one model structural framework, so exploration of other structures and models is an important next step to generate a fuller picture of overall uncertainty.

The conclusions we reach about the relative importance of different parameters are dependent upon the estimated ranges of the parameters from the expert elicitation. If it is decided that a parameter is actually less uncertain than we have assumed, then the variance analysis can easily be repeated using the emulators and a new ranking of important parameters obtained. However, if the model structures or design of the parameterisations changes, then new model runs would have to be performed unless new model processes simply help to constrain the value of the existing parameters.

How can these results be related to uncertainty in aerosol forcing? We have quantified uncertainties in present-day CCN, but the overall uncertainty in the indirect effect is determined by the uncertainty in CCN as well as uncertainties in cloud occurrence and cloud-related processes (updraught speeds, precipitation processes, etc). Because aerosol forcing is calculated relative to some baseline (such as the pre-industrial era) the uncertainty in forcing also depends on the baseline (e.g. pre-industrial) CCN concentration. In fact, as we showed in Schmidt et al. (2012) the cloud albedo forcing will probably be more sensitive to the uncertainties in the pre-industrial CCN than to the present-day CCN. Thus, the ranking of important parameters for forcing may differ from what we have presented here.

Acknowledgements. We acknowledge funding from the Natural Environment Research Council AEROS project under grant NE/G006172/1 and the EU FP7 IP PEGASOS (FP7-ENV-2010/265148). We would also like to thank several colleagues who provided informal input to the expert elicitation process: Mathew Evans, Hugo Denier van der Gon, HC Hansson, Matthew Woodhouse, Helen Macintyre, Joonas Merikanto, Anja Schmidt, Martyn Chipperfield, Steve Arnold.

Title Page

Abstract

Introduction

Conclusions

References

Tables

Figures

◀

▶

◀

▶

Back

Close

Full Screen / Esc

Printer-friendly Version

Interactive Discussion



Lindsay, K., Matthews, H. D., Raddatz, T., Rayner, P., Reick, C., Roeckner, E., Schnitzler, K. - G., Schnur, R., Strassmann, K., Weaver, A. J., Yoshikawa, C., and Zeng, N.: Climate-carbon cycle feedback analysis: results from the C4MIP model intercomparison, *J. Climate*, 19, 3337–3353, 2006. 6298

5 Gates, W. L., Boyle, J. S., Covey, C., Dease, C. G., Doutriaux, C. M., Drach, R. S., Fiorino, M., Gleckler, P. J., Hnilo, J. J., Marlais, S. M., Phillips, T. J., Potter, G. L., Santer, B. D., Sperber, K. R., Taylor, K. E., and Williams, D. N.: An overview of the results of the Atmospheric Model Intercomparison Project (AMIP I), *B. Am. Meteor. Soc.*, 73, 1962–1970, 1998. 6298

10 Ghan, S., Laulainen, N., Easter, R., Wagener, R., Nemesure, S., Chapman, E., Zhang, Y., and Leung, R.: Evaluation of aerosol direct radiative forcing in MIRAGE, *J. Geophys. Res.*, 106, 5295–5316, 2001. 6297

Ghan, S. J. and Schwartz, S. E.: Aerosol properties and processes, *B. Am. Meteor. Soc.*, 88, 1059–1083, 2007. 6297

15 Giorgi, F.: Dry deposition velocities of atmospheric aerosols as inferred by applying a particle dry deposition parameterization to a general circulation model, *Tellus B*, 40, 23–41, doi:10.1111/j.1600-0889.1988.tb00210.x, 1988. 6316

Gurciullo, C. S. and Pandis, S. N.: Effect of composition variations in cloud droplet populations on aqueous-phase chemistry, *J. Geophys. Res.*, 102, 9375–9385, doi:10.1029/96JD03651, 1997. 6314

20 Haerter, J. O., Roeckner, E., Tomassini, L., and von Storch, J. S.: Parametric uncertainty effects on aerosol radiative forcing, *Geophys. Res. Lett.*, 36, L15707, doi:10.1029/2009GL039050, 2009. 6299

25 Haylock, R. G. and O'Hagan, A.: On inference for outputs of computationally expensive algorithms with uncertainty on the inputs, in: *Bayesian Statistics 5*, edited by: Bernardo, J. M., Berger, J. O., Dawid, A. P., and Smith, A. F. M., Oxford University Press, Oxford, 629–637, 1996. 6304

Haywood, A. M., Dowsett, H. J., Otto-Bliesner, B., Chandler, M. A., Dolan, A. M., Hill, D. J., Lunt, D. J., Robinson, M. M., Rosenbloom, N., Salzmann, U., and Sohl, L. E.: Pliocene Model Intercomparison Project (PlioMIP): experimental design and boundary conditions (Experiment 1), *Geosci. Model Dev.*, 3, 227–242, doi:10.5194/gmd-3-227-2010, 2010. 6298

30 Heald, C. L., Coe, H., Jimenez, J. L., Weber, R. J., Bahreini, R., Middlebrook, A. M., Russell, L. M., Jolleys, M., Fu, T.-M., Allan, J. D., Bower, K. N., Capes, G., Crosier, J., Morgan, W. T., Robinson, N. H., Williams, P. I., Cubison, M. J., DeCarlo, P. F., and Dunlea, E. J.:

Global CCN
uncertainty

L. A. Lee et al.

Title Page

Abstract

Introduction

Conclusions

References

Tables

Figures

I◀

▶I

◀

▶

Back

Close

Full Screen / Esc

Printer-friendly Version

Interactive Discussion



An AeroCom initial assessment – optical properties in aerosol component modules of global models, *Atmos. Chem. Phys.*, 6, 1815–1834, doi:10.5194/acp-6-1815-2006, 2006. 6298

Koch, D., Schulz, M., Kinne, S., McNaughton, C., Spackman, J. R., Balkanski, Y., Bauer, S., Berntsen, T., Bond, T. C., Boucher, O., Chin, M., Clarke, A., De Luca, N., Dentener, F., Diehl, T., Dubovik, O., Easter, R., Fahey, D. W., Feichter, J., Fillmore, D., Freitag, S., Ghan, S., Ginoux, P., Gong, S., Horowitz, L., Iversen, T., Kirkevåg, A., Klimont, Z., Kondo, Y., Krol, M., Liu, X., Miller, R., Montanaro, V., Moteki, N., Myhre, G., Penner, J. E., Perlwitz, J., Pitari, G., Reddy, S., Sahu, L., Sakamoto, H., Schuster, G., Schwarz, J. P., Seland, Ø., Stier, P., Takegawa, N., Takemura, T., Textor, C., van Aardenne, J. A., and Zhao, Y.: Evaluation of black carbon estimations in global aerosol models, *Atmos. Chem. Phys.*, 9, 9001–9026, doi:10.5194/acp-9-9001-2009, 2009. 6298

Kokkola, H., Korhonen, H., Lehtinen, K. E. J., Makkonen, R., Asmi, A., Järvenoja, S., Anttila, T., Partanen, A.-I., Kulmala, M., Järvinen, H., Laaksonen, A., and Kerminen, V.-M.: SALSA – a Sectional Aerosol module for Large Scale Applications, *Atmos. Chem. Phys.*, 8, 2469–2483, doi:10.5194/acp-8-2469-2008, 2008. 6343

Korhonen, H., Carslaw, K. S., Spracklen, D. V., Ridley, D. A., and Ström, J.: A global model study of processes controlling aerosol size distributions in the Arctic spring and summer, *J. Geophys. Res.*, 113, D08211, doi:10.1029/2007JD009114, 2008. 6309, 6316, 6332, 6338

Kravitz, B., Robock, A., Boucher, O., Schmidt, H., Taylor, K. E., Stenchikov, G., and Schulz, M.: The geoengineering model intercomparison project (GeoMIP), *Atmos. Sci. Lett.*, 12, 162–167, 2011. 6298

Kreidenweis, S. M., Walcek, C. J., Feingold, G., Gong, W., Jacobson, M. Z., Kim, C.-H., Liu, X., Penner, J. E., Nenes, A., and Seinfeld, J. H.: Modification of aerosol mass and size distribution due to aqueous-phase SO₂ oxidation in clouds: Comparisons of several models, *J. Geophys. Res.*, 108, 4213, doi:10.1029/2002JD002697, 2003. 6314

Kuang, C., McMurry, P. H., McCormick, A. V., and Eisele, F. L.: Dependence of nucleation rates on sulfuric acid vapor concentration in diverse atmospheric locations, *J. Geophys. Res.*, 113, D10209, doi:10.1029/2007JD009253, 2008. 6313

Kulmala, M., Hämeri, K., Aalto, P. P., Mäkelä, J. M., Pirjola, L., Nilsson, E. D., Buzorius, G., Rannik, Ü., Dal Maso, M., Seidl, W., Hoffman, T., Janson, R., Hansson, H. C., Viisanen, Y., Laaksonen, A., and O'Dowd, C. D.: Overview of the international project on biogenic aerosol formation in the boreal forest (BIOFOR), *Tellus B*, 53, 324–343, 2003. 6337

- Kulmala, M., Lehtinen, K. E. J., and Laaksonen, A.: Cluster activation theory as an explanation of the linear dependence between formation rate of 3nm particles and sulphuric acid concentration, *Atmos. Chem. Phys.*, 6, 787–793, doi:10.5194/acp-6-787-2006, 2006. 6313
- Lauer, A., Hendricks, J., Ackermann, I., Schell, B., Hass, H., and Metzger, S.: Simulating aerosol microphysics with the ECHAM/MADE GCM – Part I: Model description and comparison with observations, *Atmos. Chem. Phys.*, 5, 3251–3276, doi:10.5194/acp-5-3251-2005, 2005. 6297
- Lee, L. A., Carslaw, K. S., Pringle, K. J., Mann, G. W., and Spracklen, D. V.: Emulation of a complex global aerosol model to quantify sensitivity to uncertain parameters, *Atmos. Chem. Phys.*, 11, 12253–12273, doi:10.5194/acp-11-12253-2011, 2011. 6300
- Lee, L. A., Carslaw, K. S., Pringle, K. J., and Mann, G. W.: Mapping the uncertainty in global CCN using emulation, *Atmos. Chem. Phys.*, 12, 9739–9751, doi:10.5194/acp-12-9739-2012, 2012. 6300, 6304, 6309, 6322, 6327
- Liu, X., Penner, J. E., and Herzog, M.: Global modeling of aerosol dynamics: Model description, evaluation, and interactions between sulfate and nonsulfate aerosols, *J. Geophys. Res.*, 110, D18206, doi:10.1029/2004JD005674, 2005. 6297
- Lohmann, U. and Feichter, J.: Global indirect aerosol effects: a review, *Atmos. Chem. Phys.*, 5, 715–737, doi:10.5194/acp-5-715-2005, 2005. 6297
- Lohmann, U. and Ferrachat, S.: Impact of parametric uncertainties on the present-day climate and on the anthropogenic aerosol effect, *Atmos. Chem. Phys.*, 10, 11373–11383, doi:10.5194/acp-10-11373-2010, 2010. 6299
- Luo, G. and Yu, F.: Sensitivity of global cloud condensation nuclei concentrations to primary sulfate emission parameterizations, *Atmos. Chem. Phys.*, 11, 1949–1959, doi:10.5194/acp-11-1949-2011, 2011. 6318
- Makkonen, R., Asmi, A., Korhonen, H., Kokkola, H., Järvenoja, S., Räisänen, P., Lehtinen, K. E. J., Laaksonen, A., Kerminen, V.-M., Järvinen, H., Lohmann, U., Bennartz, R., Feichter, J., and Kulmala, M.: Sensitivity of aerosol concentrations and cloud properties to nucleation and secondary organic distribution in ECHAM5-HAM global circulation model, *Atmos. Chem. Phys.*, 9, 1747–1766, doi:10.5194/acp-9-1747-2009, 2009. 6344
- Makkonen, R., Asmi, A., Kerminen, V.-M., Boy, M., Arneth, A., Hari, P., and Kulmala, M.: Air pollution control and decreasing new particle formation lead to strong climate warming, *Atmos. Chem. Phys.*, 12, 1515–1524, doi:10.5194/acp-12-1515-2012, 2012. 6342

Global CCN
uncertainty

L. A. Lee et al.

Title Page

Abstract

Introduction

Conclusions

References

Tables

Figures

I◀

▶I

◀

▶

Back

Close

Full Screen / Esc

Printer-friendly Version

Interactive Discussion



Global CCN
uncertainty

L. A. Lee et al.

Title Page

Abstract

Introduction

Conclusions

References

Tables

Figures

I◀

▶I

◀

▶

Back

Close

Full Screen / Esc

Printer-friendly Version

Interactive Discussion



the role of organics in aerosol particle formation under atmospheric conditions, *Proc. Natl. Acad. Sci.*, 107, 6646–6651, doi:10.1073/pnas.0911330107, 2010. 6313, 6332

Nenes, A. and Seinfeld, J. H.: Parameterization of cloud droplet formation in global climate models, *J. Geophys. Res.*, 108, 4415, doi:10.1029/2002JD002911, 2003. 6314

5 Nightingale, P. D., Liss, P. S., and Schlosser, P.: Measurements of air-sea gas transfer during an open ocean algal bloom, *Geophys. Res. Lett.*, 27, 2117–2120, 2000. 6319

Oakley, J. E. and O'Hagan, A.: SHELF: the Sheffield Elicitation Framework (version 2.0), <http://tonyohagan.co.uk/shelf>, school of Mathematics and Statistics, University of Sheffield, UK, 2010. 6302, 6303

10 O'Dowd, C. D. and de Leeuw, G.: Marine aerosol production: a review of the current knowledge, *Philos. T. R. Soc. A*, 365, 1753–1774, 2007. 6319

O'Hagan, A.: Bayesian analysis of computer code outputs: a tutorial, *Reliab. Eng. Syst. Safety*, 91, 1290–1300, 2006. 6304

15 O'Hagan, A., Buck, C. E., Daneshkhah, A., Eiser, J. R., Garthwaite, P. H., Jenkinson, D. J., Oakley, J. E., and Rakow, T.: *Uncertain Judgements: Eliciting Expert Probabilities*, Wiley, Chichester, 2006. 6301

Pan, W., Tatang, M. A., McRae, G. J., and Prinn, R. G.: Uncertainty analysis of direct radiative forcing by anthropogenic sulfate aerosols, *J. Geophys. Res.*, 102, 21915–21924, 1997. 6299

20 Partridge, D. G., Vrugt, J. A., Tunved, P., Ekman, A. M. L., Struthers, H., and Sorooshian, A.: Inverse modelling of cloud-aerosol interactions – Part 2: Sensitivity tests on liquid phase clouds using a Markov chain Monte Carlo based simulation approach, *Atmos. Chem. Phys.*, 12, 2823–2847, doi:10.5194/acp-12-2823-2012, 2012. 6299

25 Penner, J. E., Andreae, M., Annegarn, H., Barrie, L., Feichter, J., Hegg, D., Jayaraman, A., Leaitch, R., Murphy, D., Nganga, J., and Pitar, G.: Aerosols, their Direct and Indirect Effects, in: *Climate Change 2001: The Scientific Basis, Contribution of Working Group I to the Third Assessment Report of the Intergovernmental Panel on Climate Change*, edited by: Houghton, J. T., Ding, Y., Griggs, D. J., Noguer, M., van der Linden, P. J., Dai, X., Maskell, K., and Johnson, C. A., Cambridge University Press, Cambridge, United Kingdom and New York, NY, USA, 2001. 6297

30 Pierce, J. R. and Adams, P. J.: Global evaluation of CCN formation by direct emission of sea salt and growth of ultrafine sea salt, *J. Geophys. Res.*, 111, D06203, doi:10.1029/2005JD006186, 2006. 6318, 6319

- Pierce, J. R. and Adams, P. J.: Efficiency of cloud condensation nuclei formation from ultrafine particles, *Atmos. Chem. Phys.*, 7, 1367–1379, doi:10.5194/acp-7-1367-2007, 2007. 6340
- Pierce, J. R. and Adams, P. J.: Uncertainty in global CCN concentrations from uncertain aerosol nucleation and primary emission rates, *Atmos. Chem. Phys.*, 9, 1339–1356, doi:10.5194/acp-9-1339-2009, 2009. 6342
- Pringle, K. J., Carslaw, K. S., Spracklen, D. V., Mann, G. M., and Chipperfield, M. P.: The relationship between aerosol and cloud drop number concentrations in a global aerosol microphysics model, *Atmos. Chem. Phys.*, 9, 4131–4144, doi:10.5194/acp-9-4131-2009, 2009. 6314
- Pujol, G., Iouss, B., and Janon, A.: Sensitivity: sensitivity analysis, R package version 1.6, available online at: <http://CRAN.R-project.org/package=sensitivity> (last access: 27 February 2013), 2008. 6308
- Reddington, C. L., Carslaw, K. S., Spracklen, D. V., Frontoso, M. G., Collins, L., Merikanto, J., Minikin, A., Hamburger, T., Coe, H., Kulmala, M., Aalto, P., Flentje, H., Plass-Dülmer, C., Birmili, W., Wiedensohler, A., Wehner, B., Tuch, T., Sonntag, A., O'Dowd, C. D., Jennings, S. G., Dupuy, R., Baltensperger, U., Weingartner, E., Hansson, H.-C., Tunved, P., Laj, P., Sellegri, K., Boulon, J., Putaud, J.-P., Gruening, C., Swietlicki, E., Roldin, P., Henzing, J. S., Moerman, M., Mihalopoulos, N., Kouvarakis, G., Ždímal, V., Zíková, N., Marinoni, A., Bonasoni, P., and Duchi, R.: Primary versus secondary contributions to particle number concentrations in the European boundary layer, *Atmos. Chem. Phys.*, 11, 12007–12036, doi:10.5194/acp-11-12007-2011, 2011. 6309, 6318, 6338
- Riipinen, I., Sihto, S.-L., Kulmala, M., Arnold, F., Dal Maso, M., Birmili, W., Saarnio, K., Teinilä, K., Kerminen, V.-M., Laaksonen, A., and Lehtinen, K. E. J.: Connections between atmospheric sulphuric acid and new particle formation during QUEST III–IV campaigns in Heidelberg and Hyytiälä, *Atmos. Chem. Phys.*, 7, 1899–1914, doi:10.5194/acp-7-1899-2007, 2007. 6313
- Rossow, W. B. and Schiffer, R. A.: Advances in understanding clouds from ISCCP, *B. Am. Meteor. Soc.*, 80, 2261–2288, 1999. 6311, 6324
- Roustant, O., Ginsbourger, D., and Deville, Y.: DiceKriging, DiceOptim: Two R Packages for the Analysis of Computer Experiments by Kriging-Based Metamodeling and Optimization, available at: <http://CRAN.R-project.org/package=DiceKriging>, *J. Stat. Softw.*, 55, 1–55, 2012. 6307

ACPD

13, 6295–6378, 2013

Global CCN
uncertainty

L. A. Lee et al.

Title Page

Abstract

Introduction

Conclusions

References

Tables

Figures

I◀

▶I

◀

▶

Back

Close

Full Screen / Esc

Printer-friendly Version

Interactive Discussion



Global CCN
uncertainty

L. A. Lee et al.

Title Page

Abstract

Introduction

Conclusions

References

Tables

Figures

I◀

▶I

◀

▶

Back

Close

Full Screen / Esc

Printer-friendly Version

Interactive Discussion



Saltelli, A., Tarantola, S., and Chan, K. P.-S.: A quantitative model-independent method for global sensitivity analysis of model output, *Technometrics*, 41, 39–56, doi:10.2307/1270993, 1999. 6308

Saltelli, A., Chan, K., and Scott, M. E.: *Sensitivity Analysis*, Wiley, New York, USA, 2000. 6308

Schimel, D., Alves, D., Enting, I., Heimann, M., Joos, F., Raynaud, D., Wigley, T., Prather, M., Derwent, R., Ehhalt, D., Fraser, P., Sanhueza, E., Zhou, X., Jonas, P., Charlson, R., Rodhe, H., Sadasivan, S., Shine, K. P., Fouquart, Y., Ramaswamy, V., Solomon, S., Srinivasan, J., Albritton, D., Isaksen, I., Lal, M., and Wuebbles, D.: Radiative forcing of climate change, in: *Climate Change 1996, Contribution of Working Group I to the 2nd Assessment Report of the Intergovernmental Panel on Climate Change*, edited by: Houghton, J. T., Meira Filho, L. G., Callander, B. A., Harris, N., Kattenberg, A., and Maskell, K., Cambridge University Press, Cambridge, United Kingdom and New York, NY, USA, 1996. 6297

Schmidt, A., Carslaw, K. S., Mann, G. W., Wilson, M., Breider, T. J., Pickering, S. J., and Thordarson, T.: The impact of the 1783–1784 AD Laki eruption on global aerosol formation processes and cloud condensation nuclei, *Atmos. Chem. Phys.*, 10, 6025–6041, doi:10.5194/acp-10-6025-2010, 2010. 6309

Schmidt, A., Ostro, B., Carslaw, K. S., Wilson, M., Thordarson, T., Mann, G. W., and Simons, A. J.: Excess mortality in Europe following a future Laki-style Icelandic eruption, *Proc. Natl. Acad. Sci.*, 108, 15710–15715, 2011. 6309

Schmidt, A., Carslaw, K. S., Mann, G. W., Rap, A., Pringle, K. J., Spracklen, D. V., Wilson, M., and Forster, P. M.: Importance of tropospheric volcanic aerosol for indirect radiative forcing of climate, *Atmos. Chem. Phys.*, 12, 7321–7339, doi:10.5194/acp-12-7321-2012, 2012. 6309, 6310, 6319, 6331, 6345

Schulz, M., Textor, C., Kinne, S., Balkanski, Y., Bauer, S., Bernsten, T., Berglen, T., Boucher, O., Dentener, F., Guibert, S., Isaksen, I. S. A., Iversen, T., Koch, D., Kirkevåg, A., Liu, X., Montanaro, V., Myhre, G., Penner, J. E., Pitari, G., Reddy, S., Seland, Ø., Stier, P., and Takemura, T.: Radiative forcing by aerosols as derived from the AeroCom present-day and pre-industrial simulations, *Atmos. Chem. Phys.*, 6, 5225–5246, doi:10.5194/acp-6-5225-2006, 2006. 6298

Seinfeld, J. H. and Pandis, S. N.: *Atmospheric Chemistry and Physics: From Air Pollution to Climate Change*, Wiley-Interscience Publication, New York, NY, 1998. 6314

Shindell, D. T., Chin, M., Dentener, F., Doherty, R. M., Faluvegi, G., Fiore, A. M., Hess, P., Koch, D. M., MacKenzie, I. A., Sanderson, M. G., Schultz, M. G., Schulz, M., Stevenson, D. S., Teich, H., Textor, C., Wild, O., Bergmann, D. J., Bey, I., Bian, H., Cuvelier, C., Dun-

can, B. N., Folberth, G., Horowitz, L. W., Jonson, J., Kaminski, J. W., Marmer, E., Park, R., Pringle, K. J., Schroeder, S., Szopa, S., Takemura, T., Zeng, G., Keating, T. J., and Zuber, A.: A multi-model assessment of pollution transport to the Arctic, *Atmos. Chem. Phys.*, 8, 5353–5372, doi:10.5194/acp-8-5353-2008, 2008. 6298

5 Sihto, S.-L., Kulmala, M., Kerminen, V.-M., Dal Maso, M., Petäjä, T., Riipinen, I., Korhonen, H., Arnold, F., Janson, R., Boy, M., Laaksonen, A., and Lehtinen, K. E. J.: Atmospheric sulphuric acid and aerosol formation: implications from atmospheric measurements for nucleation and early growth mechanisms, *Atmos. Chem. Phys.*, 6, 4079–4091, doi:10.5194/acp-6-4079-2006, 2006. 6313

10 Slinn, W. G. N.: Predictions for particle deposition to vegetative canopies, *Atmos. Environ.*, 16, 1785–1794, 1982. 6316

Spracklen, D. V., Pringle, K. J., Carslaw, K. S., Chipperfield, M. P., and Mann, G. W.: A global off-line model of size-resolved aerosol microphysics: I. Model development and prediction of aerosol properties, *Atmos. Chem. Phys.*, 5, 2227–2252, doi:10.5194/acp-5-2227-2005, 2005a. 6297, 6309, 6312, 6314

15 Spracklen, D. V., Pringle, K. J., Carslaw, K. S., Chipperfield, M. P., and Mann, G. W.: A global off-line model of size-resolved aerosol microphysics: I I. Identification of key uncertainties, *Atmos. Chem. Phys.*, 5, 3233–3250, doi:10.5194/acp-5-3233-2005, 2005b. 6309, 6312, 6318

20 Spracklen, D. V., Carslaw, K. S., Kulmala, M., Kerminen, V.-M., Mann, G. W., and Sihto, S.-L.: The contribution of boundary layer nucleation events to total particle concentrations on regional and global scales, *Atmos. Chem. Phys.*, 6, 5631–5648, doi:10.5194/acp-6-5631-2006, 2006. 6313, 6314, 6320

25 Spracklen, D. V., Carslaw, K. S., Kulmala, M., Kerminen, V.-M., Sihto, S.-L., Riipinen, I., Merikanto, J., Mann, G. W., Chipperfield, M. P., Wiedensohler, A., Birmili, W., and Lihavainen, H.: Contribution of particle formation to global cloud condensation nuclei concentrations, *Geophys. Res. Lett.*, 35, L06 808, doi:10.1029/2007GL033038, 2008. 6297, 6320, 6344

30 Spracklen, D. V., Carslaw, K. S., Merikanto, J., Mann, G. W., Reddington, C. L., Pickering, S., Ogren, J. A., Andrews, E., Baltensperger, U., Weingartner, E., Boy, M., Kulmala, M., Laakso, L., Lihavainen, H., Kivekäs, N., Komppula, M., Mihalopoulos, N., Kouvarakis, G., Jennings, S. G., O'Dowd, C., Birmili, W., Wiedensohler, A., Weller, R., Gras, J., Laj, P., Sellegri, K., Bonn, B., Krejci, R., Laaksonen, A., Hamed, A., Minikin, A., Harrison, R. M., Talbot, R., and Sun, J.: Explaining global surface aerosol number concentrations in terms of primary

Takemura, T., and Tie, X.: Analysis and quantification of the diversities of aerosol life cycles within AeroCom, *Atmos. Chem. Phys.*, 6, 1777–1813, doi:10.5194/acp-6-1777-2006, 2006. 6298

5 Textor, C., Schulz, M., Guibert, S., Kinne, S., Balkanski, Y., Bauer, S., Berntsen, T., Berglen, T., Boucher, O., Chin, M., Dentener, F., Diehl, T., Feichter, J., Fillmore, D., Ginoux, P., Gong, S., Grini, A., Hendricks, J., Horowitz, L., Huang, P., Isaksen, I. S. A., Iversen, T., Kloster, S., Koch, D., Kirkevåg, A., Kristjansson, J. E., Krol, M., Lauer, A., Lamarque, J. F., Liu, X., Montanaro, V., Myhre, G., Penner, J. E., Pitari, G., Reddy, M. S., Seland, Ø., Stier, P., Takemura, T., and Tie, X.: The effect of harmonized emissions on aerosol properties in global models – an
10 AeroCom experiment, *Atmos. Chem. Phys.*, 7, 4489–4501, doi:10.5194/acp-7-4489-2007, 2007. 6298

Tiedtke, M.: A comprehensive mass flux scheme for cumulus parameterization in large scale models, *Mon. Weather Rev.*, 117, 1779–1800, 1989. 6310

Twomey, S.: Aerosols, clouds and radiation, *Atmos. Environ.*, 25, 2435–2442, doi:10.1016/0960-1686(91)90159-5, 1991. 6322

15 Uppala, S. M., Kållberg, P. W., Simmons, A. J., Andrae, U., Bechtold, V., Fiorino, M., Gibson, J. K., Haseler, J., Hernandez, A., Kelly, G. A., Li, X., Onogi, K., Saarinen, S., Sokka, N., Allan, R. P., Andersson, E., Arpe, K., Balmaseda, M. A., Beljaars, A. C. M., Van De Berg, L., Bidlot, J., Bormann, N., Caires, S., Chevallier, F., Dethof, A., Dragosavac, M., Fisher, M., Fuentes, M., Hagemann, S., Holm, E., Hoskins, B. J., Isaksen, L., Janssen, P. A. E. M., Jenne, R., McNally, A. P., Mahfouf, J. F., Morcrette, J. J., Rayner, N. A., Saunders, R. W., Simon, P., Sterl, A., Trenberth, K. E., Untch, A., Vasiljevic, D., Viterbo, P., and Woollen, J.:
20 The ERA-40 re-analysis, *Q. J. Roy. Meteorol. Soc.*, 131, 2961–3012, 2005. 6309

Van der Werf, G. R., Randerson, J. T., Collatz, G. J., and Giglio, L.: Carbon emissions from fires in tropical and subtropical ecosystems, *Glob. Change Biol.*, 9, 547–562, 2003. 6317

Vehkamäki, H., Kulmala, M., Napari, I., Lehtinen, K. E. J., Timmreck, C., Noppel, M., and Laaksonen, A.: An improved parameterization for sulfuric acid-water nucleation rates for tropospheric and stratospheric conditions, *J. Geophys. Res.*, 107, 4622, doi:10.1029/2002JD002184, 2002. 6311, 6312

30 Weisenstein, D. K., Penner, J. E., Herzog, M., and Liu, X.: Global 2-D intercomparison of sectional and modal aerosol modules, *Atmos. Chem. Phys.*, 7, 2339–2355, doi:10.5194/acp-7-2339-2007, 2007. 6343

Title Page

Abstract

Introduction

Conclusions

References

Tables

Figures

I ◀

▶ I

◀

▶

Back

Close

Full Screen / Esc

Printer-friendly Version

Interactive Discussion

**Table 1.** The uncertain parameters and emissions factors

Parameter Key	Parameter name	Description of parameter	Uncertainty range	Effect
P1	BL_NUC	Boundary layer nucleation rate coeff (A)	$1e^{-10}$ – $2e^{-4}$ s ⁻¹	Absolute
P2	FT_NUC	Free troposphere nucleation rate	0.01–10	Scaled
P3	AGEING	Ageing “rate” from insoluble to soluble	0.3–5 monolayer	Absolute
P4	ACT_DIAM	Cloud drop activation dry diameter	50–100 nm	Absolute
P5	SO2O3_CLEAN	pH of cloud drops (controls SO ₂ + O ₃)	pH 4–6.5	Absolute
P6	SO2O3_POLL	pH of cloud drops (SO ₂ + O ₃)	pH 3.5–5	Absolute
P7	NUC_SCAV_DIAM	Nucleation scavenging diameter offset dry diameter	0–50 nm	Absolute
P8	NUC_SCAV_ICE	Nucleation scavenging fraction (accumulation mode) in mixed and ice clouds ($T < -15$ °C)	0–1	Scaled
P9	DRYDEP_AER_AIT	Dry deposition velocity of Aitken mode aerosol	0.5–2	Scaled
P10	DRYDEP_AER_ACC	Dry deposition velocity of accumulation mode aerosol	0.1–10	Scaled
P11	ACC_WIDTH	Modal width (accumulation soluble/insoluble)	1.2–1.8	Absolute
P12	AIT_WIDTH	Modal width (Aitken soluble/insoluble)	1.2–1.8	Absolute
P13	NUCAIT_WIDTH	Mode separation diameter (nucleation/Aitken)	9–18 nm	Absolute
P14	AITACC_WIDTH	Mode separation diameter (Aitken/accumulation)	0.9 – $2 \times$ ACT_DIAM	Scaled
P15	FF_EMS	BCOC mass emission rate (fossil fuel)	0.5–2	Scaled
P16	BB_EMS	BCOC mass emission rate (biomass burning)	0.25–4	Scaled
P17	BF_EMS	BCOC mass emission rate (biofuel)	0.25–4	Scaled
P18	FF_DIAM	BCOC emitted mode diameter (fossil fuel)	30–80 nm	Absolute
P19	BB_DIAM	BCOC emitted mode diameter (biomass burning)	50–200 nm	Absolute
P20	BF_DIAM	BCOC emitted mode diameter (biofuel)	50–200 nm	Absolute
P21	PRIM_SO4_FRAC	Mass fraction of SO ₂ converted to new SO ₄ particles in sub-grid power plant plumes	0–1 %	Absolute
P22	PRIM_SO4_DIAM	Mode diameter of new sub-grid SO ₄ particles	20–100 nm	Absolute
P23	SS_ACC	Sea spray mass flux (coarse/accumulation)	0.2–5	Scaled
P24	ANTH_SO2	SO ₂ emission flux (anthropogenic)	0.6–1.5	Scaled
P25	VOLC_SO2	SO ₂ emission flux (volcanic)	0.5–2	Scaled
P26	DMS_FLUX	DMS emission flux	0.5–2	Scaled
P27	BIO_SOA	Biogenic monoterpene production of SOA	5–360 Tg a ⁻¹	Absolute
P28	ANTH_SOA	Anthropogenic VOC production of SOA	3–160 Tg a ⁻¹	Absolute

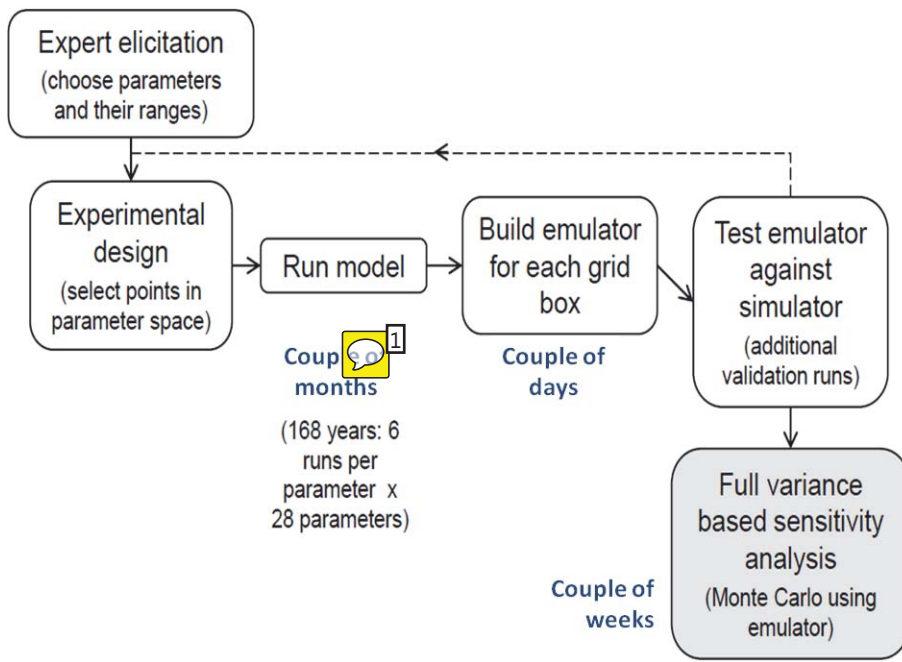


Fig. 1. The step-by-step approach to sensitivity analysis via emulation. The blue text indicates the approximate computation time.

Title Page

Abstract Introduction

Conclusions References

Tables Figures

◀ ▶

◀ ▶

Back Close

Full Screen / Esc

Printer-friendly Version

Interactive Discussion



 Number: 1 Author: reviewer Subject: Sticky Note Date: 2013-05-02 12:24:12
"Couple of months" is colloquial English. Proper language use could be "several months" or "two months".

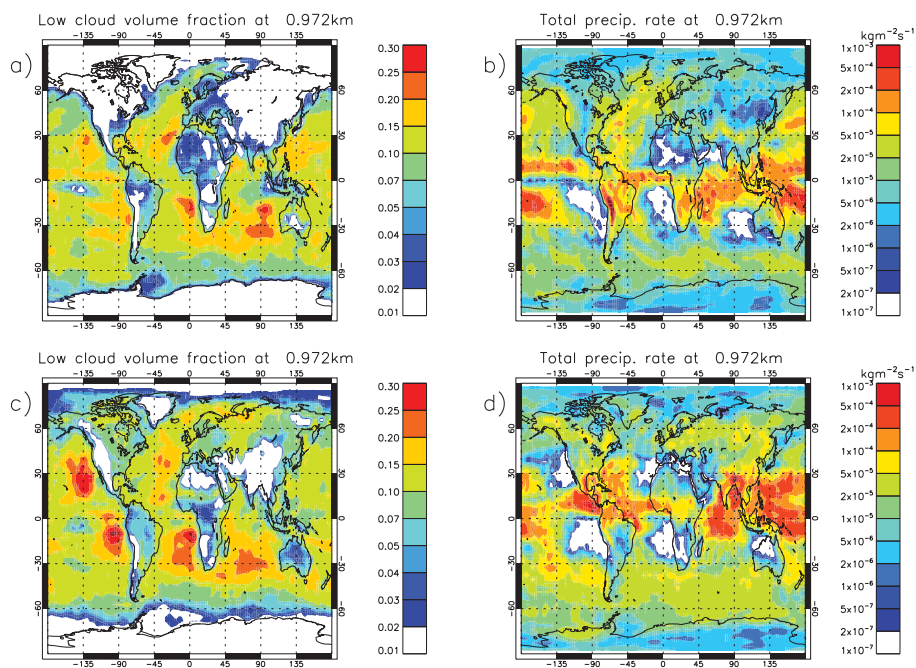


Fig. 2. Global low-level cloud volume fraction based on ISCCP global D2 all-cloud data (left column) and total (large-scale and convective-scale) modelled precipitation rate at ~ 879 hPa (right column) for January (top row) and July (bottom row).

Title Page

Abstract

Introduction

Conclusions

References

Tables

Figures

◀

▶

◀

▶

Back

Close

Full Screen / Esc

Printer-friendly Version

Interactive Discussion



Number: 1 Author: reviewer Subject: Sticky Note Date: 2013-05-02 12:24:12

Which of the uncertain parameters have the greatest impact on these results? Could some of the parameters be dropped entirely without changing the agreement between emulator and simulations?

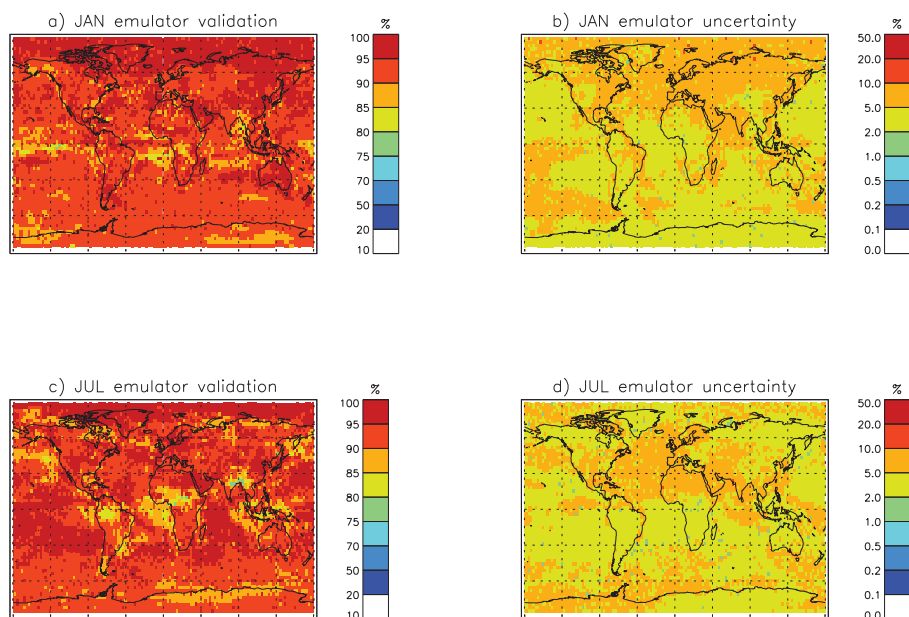


Fig. 4. Global validation of emulator-predicted CCN. CCN concentrations predicted by the emulator are compared against CCN from 84 additional GLOMAP model simulations for every model grid box on the 915 hPa model level. The fraction of GLOMAP simulations lying within the emulator 95 % confidence interval for every grid box is shown for **(a)** January and **(c)** July. In **(b)** and **(d)** the emulator uncertainty is shown as the standard deviation around the mean due to the emulator uncertainty (σ_{emulator}) divided by the standard deviation due to the uncertain parameters (σ_{CCN} , shown in Fig. 5). Thus, everywhere, the emulator uncertainty is less than 10% of the parametric uncertainty.

Title Page

Abstract

Introduction

Conclusions

References

Tables

Figures

◀

▶

◀

▶

Back

Close

Full Screen / Esc

Printer-friendly Version

Interactive Discussion



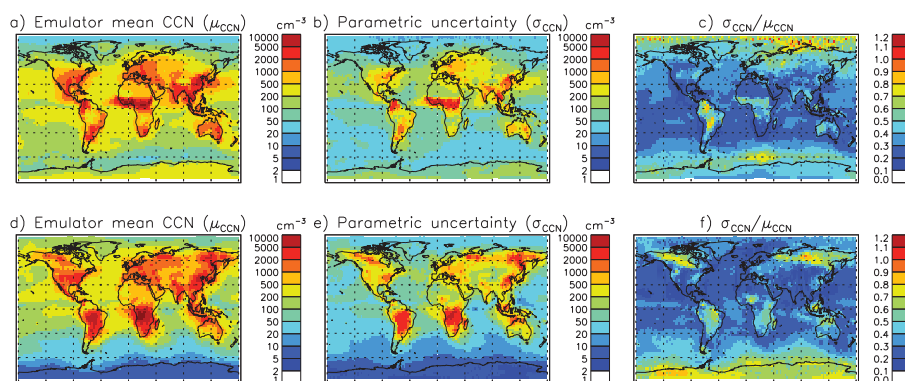


Fig. 5. Global fields of CCN concentration and associated uncertainty on the 915 hPa model level. Left column (**a** and **d**), mean CCN (μ_{CCN}) predicted by the emulators for January and July. Middle column (**b** and **e**), uncertainty in CCN (defined as the emulator standard deviation σ_{CCN} due to the uncertain parameters). Right column (**c** and **f**), coefficient of variation ($\sigma_{\text{CCN}}/\mu_{\text{CCN}}$ in each grid box).

Title Page

Abstract Introduction

Conclusions References

Tables Figures

◀ ▶

◀ ▶

Back Close

Full Screen / Esc

Printer-friendly Version

Interactive Discussion



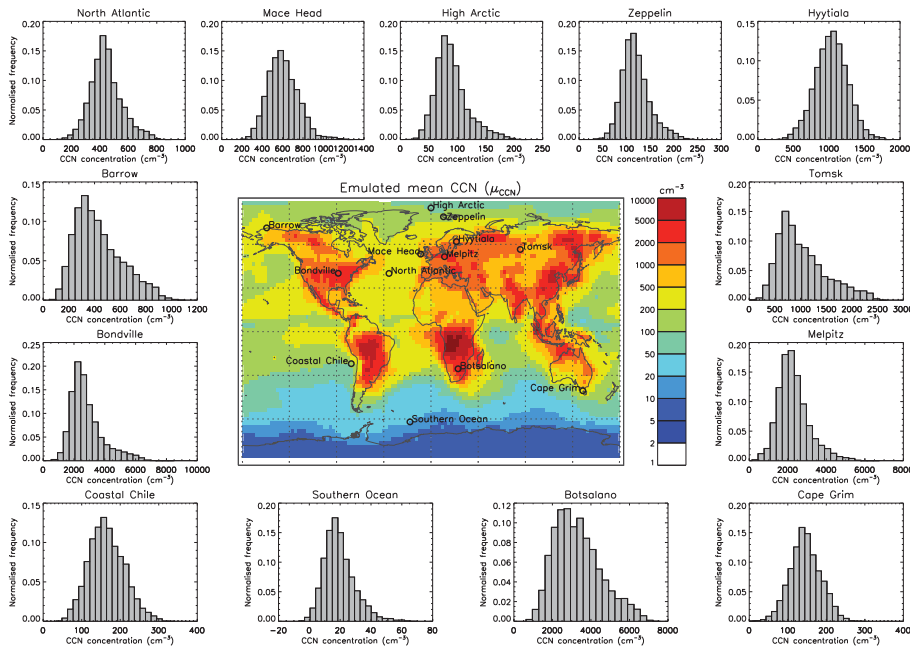


Fig. 6. The frequency distribution of CCN concentrations across the 28-dimensional parameter uncertainty space simulated from the emulators. Distributions are shown for July for 13 model grid boxes corresponding to the locations in Sect. 6.3.6 and Fig. 9. The map of mean CCN is the same as in Fig. 5. In some cases the CCN concentration is negative when in reality it will be truncated at zero meaning that the uncertainty in some places will be slightly overestimated. Since the negative CCN is confined to a small region of the parameter uncertainty space the sensitivity analysis results will be robust to the negative values. Emulator calibration is not part of this study but the first regions of parameter space to be removed will be those that give negative values.

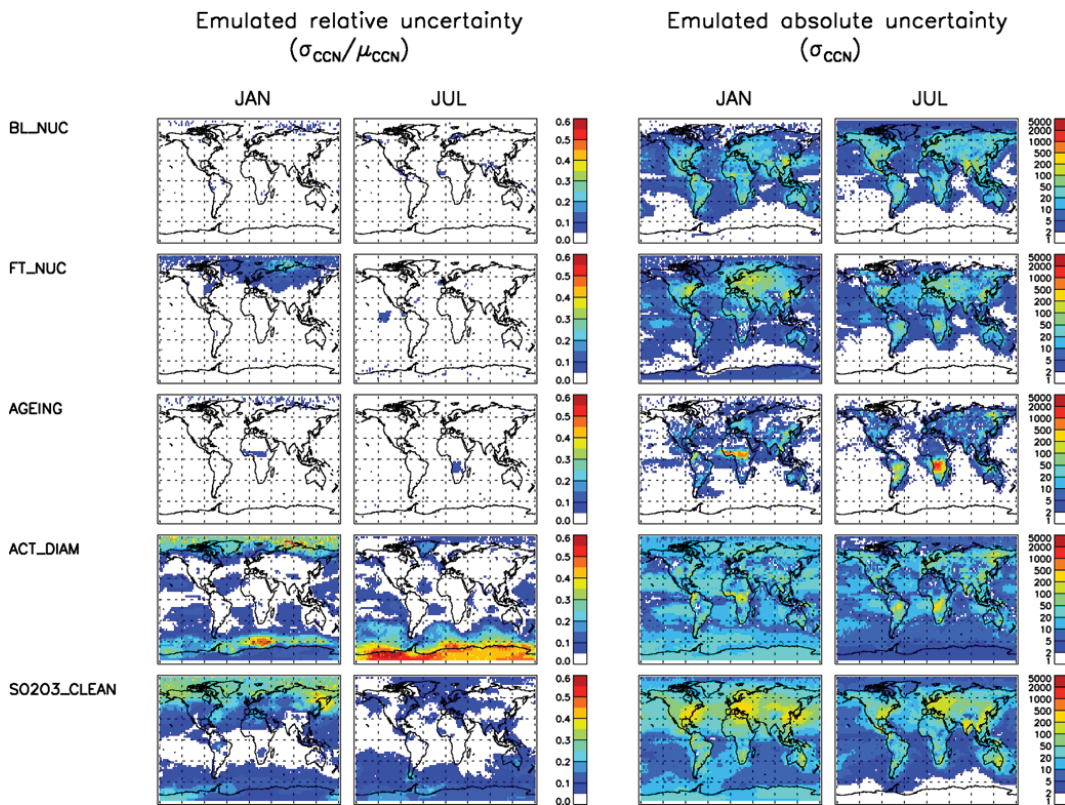


Fig. 7. The global distribution of CCN standard deviation ($\sigma_{\text{CCN},i}$, right two columns) and relative uncertainty ($\sigma_{\text{CCN},i}/\mu_{\text{CCN}}$, left two columns) for each of the 28 parameters i in Table 1 for January and July. Results are shown for the 915 hPa model level. Each map is generated from the results of 8192 independent emulators (the total number of grid boxes on one level of the model).

Title Page

Abstract

Introduction

Conclusions

References

Tables

Figures

◀

▶

◀

▶

Back

Close

Full Screen / Esc

Printer-friendly Version

Interactive Discussion



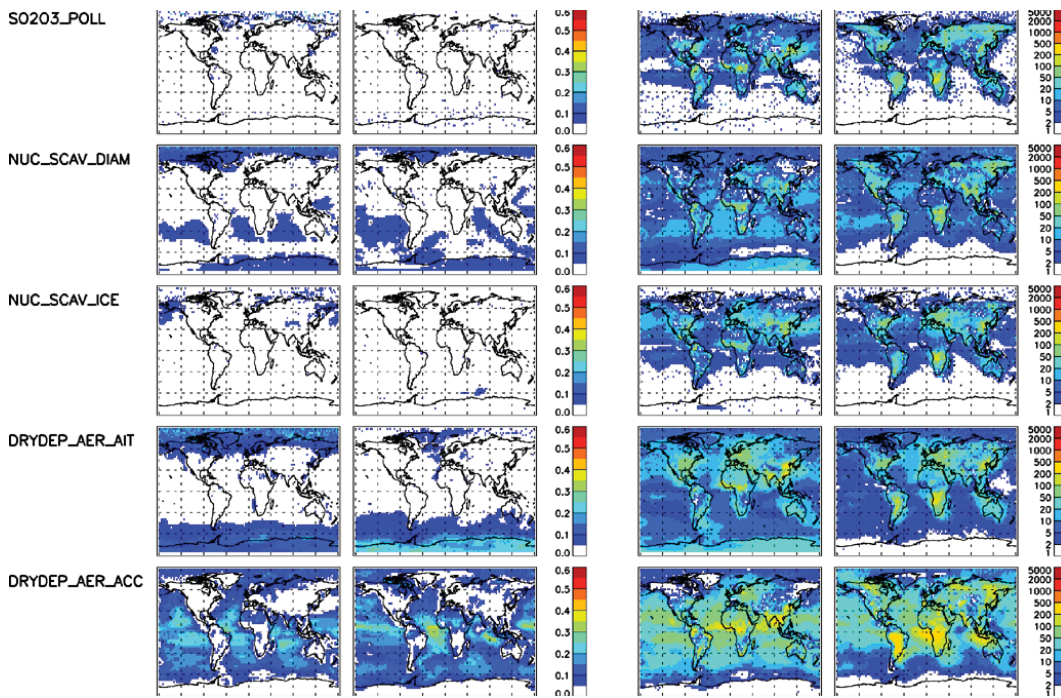


Fig. 7. Continued.

Global CCN uncertainty

L. A. Lee et al.

Title Page

Abstract Introduction

Conclusions References

Tables Figures

◀ ▶

◀ ▶

Back Close

Full Screen / Esc

Printer-friendly Version

Interactive Discussion



Global CCN uncertainty

L. A. Lee et al.

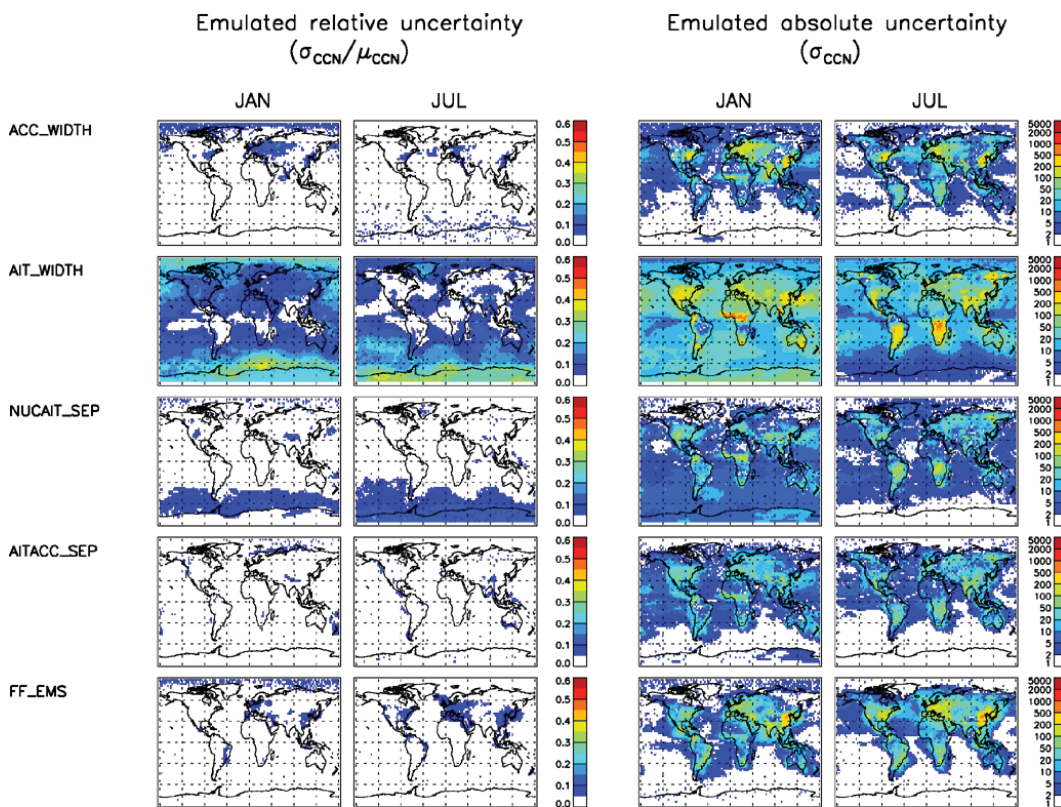


Fig. 7. Continued.

Title Page

Abstract

Introduction

Conclusions

References

Tables

Figures

◀

▶

◀

▶

Back

Close

Full Screen / Esc

Printer-friendly Version

Interactive Discussion



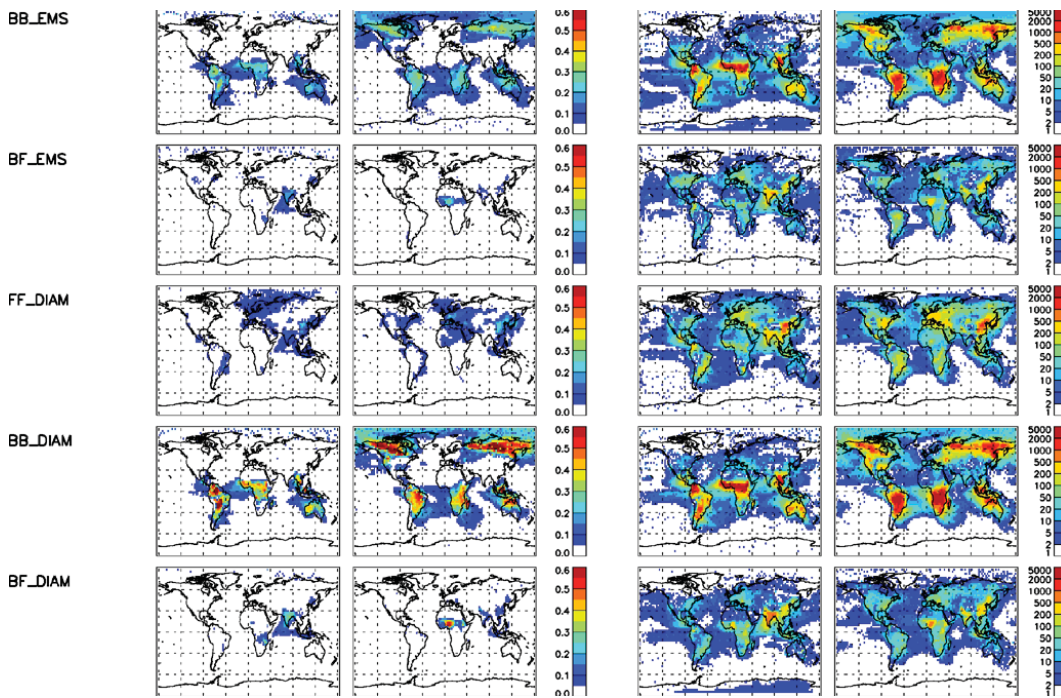


Fig. 7. Continued.

Global CCN uncertainty

L. A. Lee et al.

Title Page

Abstract Introduction

Conclusions References

Tables Figures

◀ ▶

◀ ▶

Back Close

Full Screen / Esc

Printer-friendly Version

Interactive Discussion



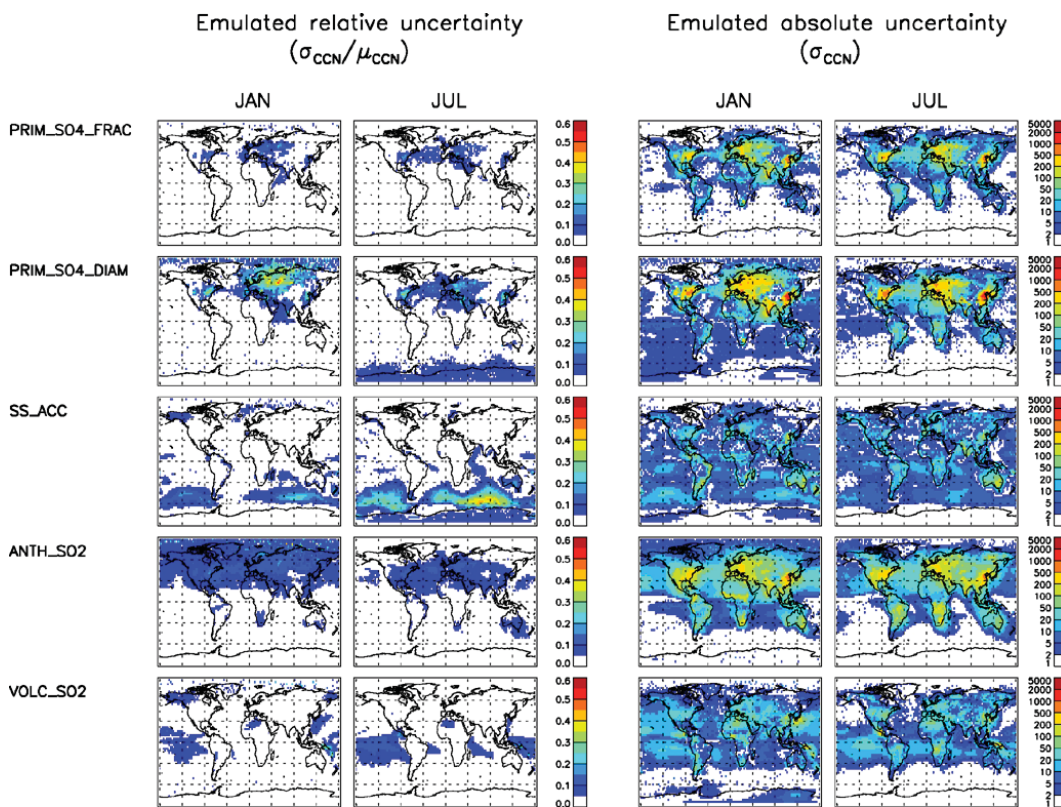


Fig. 7. Continued.

Title Page

Abstract

Introduction

Conclusions

References

Tables

Figures

◀

▶

◀

▶

Back

Close

Full Screen / Esc

Printer-friendly Version

Interactive Discussion



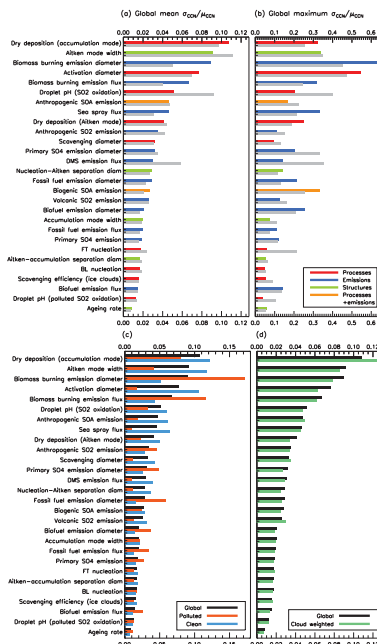


Fig. 8. Global summary of the ranked parameter uncertainties for CCN. **(a)** Global mean $\sigma_{CCN,i}/\mu_{CCN}$ where i is the parameter, calculated by globally averaging $\sigma_{CCN,i}/\mu_{CCN}$ over all grid boxes, weighting by grid-box area. The ranked uncertainties are shown in colour for July and in grey for January. The colours show the classification of the parameters according to model processes (red), emissions (blue), processes and emissions (orange) and the model structure (green). **(b)** Global maximum $\sigma_{CCN,i}/\mu_{CCN}$ calculated over a coarser grid (32×16 grid boxes) than the GLOMAP grid (128×64 grid boxes) in order to suppress noise in the data. **(c)** Stratified into polluted and clean mean $\sigma_{CCN,i}/\mu_{CCN}$ for July. Polluted is defined as $BC > 100 \text{ ng m}^{-3}$ and clean as $BC < 50 \text{ ng m}^{-3}$. The black bars are July global means from **(a)**. **(d)** Global rankings in July weighted by ISCCP global low level cloud volume fraction.

 Number: 1 Author: reviewer Subject: Sticky Note Date: 2013-05-02 12:24:12

So the value of CCN can become negative? The distributions seem to be skewed. Therefore, showing 2.sigma error bars should be replaced by a more meaningful measure of deviation from the mean, perhaps percentiles.

 Number: 2 Author: reviewer Subject: Comment on Text Date: 2013-05-02 12:24:12

This is interesting, so the interactions tend to increase the overall effect?

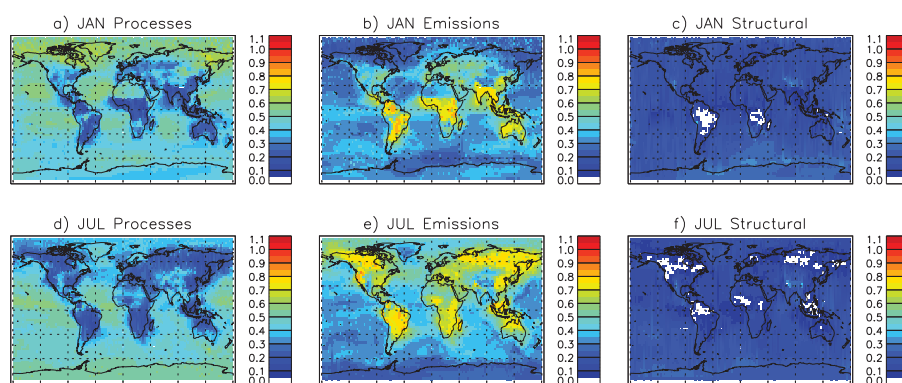


Fig. 10. The contribution to the relative uncertainty according to microphysical processes (left column), emissions (middle column) and model structures (right column) for January (top row) and July (bottom row). The relative uncertainties ($\sigma_{\text{CCN},i}/\mu_{\text{CCN}}$) for each of the 28 parameters i shown in Fig. 7 are summed according to the classification of the parameters shown in Fig. 8. The two SOA-related parameters are included in both the processes and emissions groups.

Title Page

Abstract

Introduction

Conclusions

References

Tables

Figures

◀

▶

◀

▶

Back

Close

Full Screen / Esc

Printer-friendly Version

Interactive Discussion



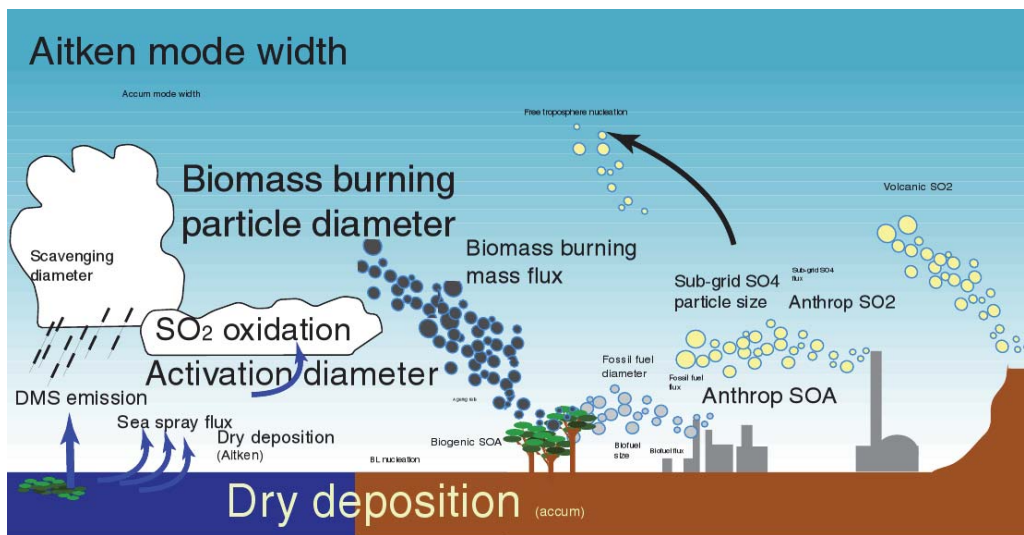


Fig. 11. Schematic showing the relative importance of the uncertain parameters for CCN. The size of the font is in direct proportion to the global and annual mean relative uncertainty.

Title Page

Abstract Introduction

Conclusions References

Tables Figures

◀ ▶

◀ ▶

Back Close

Full Screen / Esc

Printer-friendly Version

Interactive Discussion



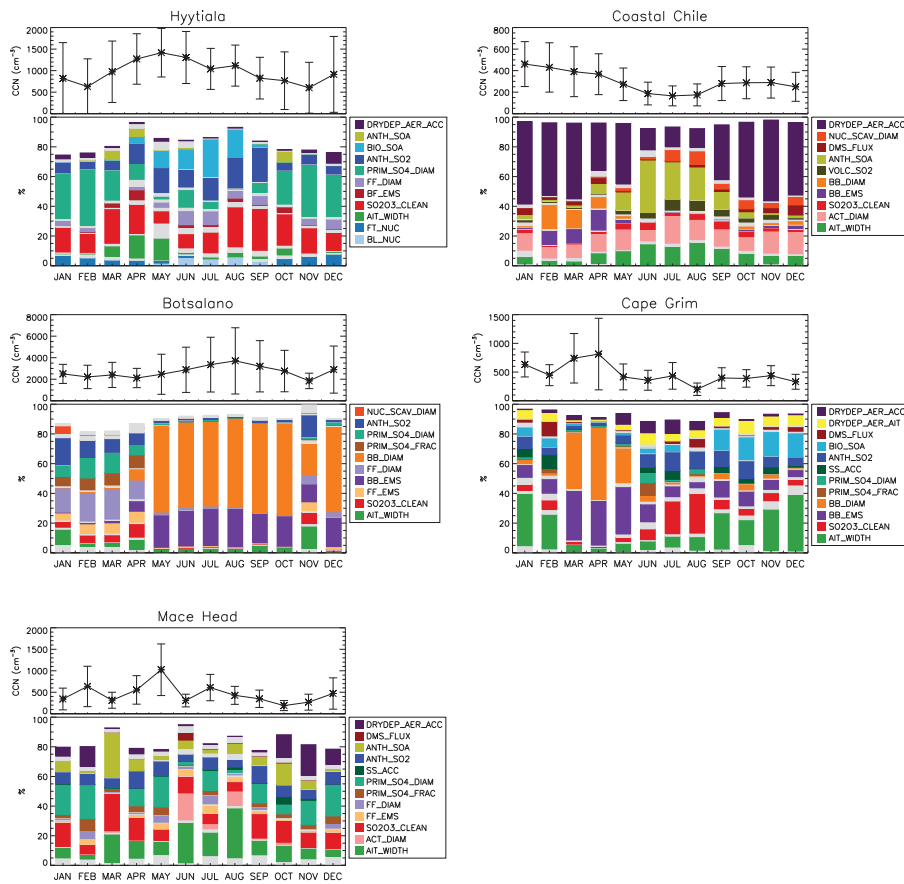


Fig. 9. Continued.

Title Page

Abstract

Introduction

Conclusions

References

Tables

Figures

◀

▶

◀

▶

Back

Close

Full Screen / Esc

Printer-friendly Version

Interactive Discussion

